

Network Inference from Co-Occurrences

Michael G. Rabbat, *Student Member, IEEE*, Mário A. T. Figueiredo, *Member, IEEE*
and Robert D. Nowak, *Member, IEEE*

Abstract—The discovery of networks is a fundamental problem arising in numerous fields of science and technology, including communication systems, biology, sociology and neuroscience. Unfortunately, it is often difficult, or impossible, to obtain data that directly reveal network structure, and so one must infer a network from incomplete data. This paper considers inferring network structure from “co-occurrence” data: observations that identify which network components (e.g., switches, routers, genes) carry each transmission but do not indicate the order in which they handle the transmission. Without order information, the number of networks that are consistent with the data grows exponentially with the size of the network (i.e., the number of nodes). Yet, the basic engineering/evolutionary principles underlying most networks strongly suggest that not all data-consistent networks are equally likely. In particular, nodes that co-occur in many observations are probably closely connected. With this in mind, we model the co-occurrence observations as independent realizations of a random walk on the network, subjected to a random permutation to account for the lack of order information. Treating permutations as missing data, we derive an *expectation-maximization* (EM) algorithm for estimating the random walk parameters. The model and EM algorithm significantly simplify the problem, but the computational complexity of the reconstruction process does grow exponentially in the length of each transmission path. For networks with long paths the exact E-step may be computationally intractable. We propose a polynomial-time *Monte Carlo EM* (MCEM) algorithm based on importance sampling and derive conditions which ensure convergence of the algorithm with high probability. Simulations and experiments with Internet measurements demonstrate the promise of this approach.

Index Terms—EM algorithm, graphical models, importance sampling, Markov models, network inference, network tomography.

I. NETWORK INFERENCE AND CO-OCCURRENCE OBSERVATIONS

The study of complex networked systems is an emerging field, impacting nearly every area of engineering and science, including the important domains of communication systems, biology, sociology, and cognitive science. The analysis of communication networks enables a better understanding of

routing, transmission patterns, and information flow [1], [2]. Characteristics of biological networks provide insight into the functional roles played by different genes, proteins, and metabolites in biological systems [3], [4]. Social network analysis can be used to gain a deeper understanding of interactions, dynamics, and the structure of organizations [5], [6]. Functional connectivity networks of brain regions are studied to better understand coupling and interaction between different neuronal colonies [7]–[9]. Obtaining or inferring the structure of networks from experimental data precedes any such analysis and is thus a basic and fundamental task, critical to many applications.

Unfortunately, measurements which directly reveal network structure are often beyond experimental capabilities or are excessively expensive. This paper considers inferring network structure from observations that identify which network components (e.g., switches, routers, genes) carry each transmission but do not indicate the order in which they handle the transmissions. Mathematically, the underlying network structure can be represented as a directed graph, and the vertices involved in each transmission form a connected subgraph. The observations only reflect which subset of vertices are involved, or “co-occur”, in each transmission; not their inter-connectivity. We refer to such observations as *co-occurrences*. Co-occurrence observations arise naturally in each of the application areas mentioned above.

Transmissions over telecommunication networks are carried by links and routers/switches which form a path between the source and terminal nodes. In some cases, it is impossible to directly observe the order in which the routers/switches handle each transmission, since sensors are geographically distributed, making precise time-synchronization impractical. The so-called *internally-sensed network tomography* problem specifically aims at recovering network structure from unordered lists of network elements along transmission paths [1].

Biological signal transduction networks describe fundamental cell functions such as growth, metabolism, differentiation, and apoptosis (disintegration) [4]. Although it is possible to test for individual, localized interactions between protein pairs, such experiments are expensive and time-consuming. High-throughput measurement techniques such as microarrays have successfully been used to identify the components of different signal transduction pathways [10]. However, microarray data only reflects order information at a very coarse, unreliable level. Developing computational techniques for inferring pathway orders is an active research area [11].

Co-occurrence or transactional data also appears in the context of social networks, e.g., by considering which academic papers are co-cited by another paper, which web pages are

This work was partially supported by *Fundação para a Ciência e Tecnologia*, Portuguese Ministry of Science and Higher Education, project POSC/EEA-CPS/61924/2004, and National Science Foundation grant CCF-0728767. The material in this paper was presented in part at the 2006 Conference on Neural Information Processing Systems, Vancouver, Canada, December 2006.

M.G. Rabbat is with the Department of Electrical and Computer Engineering, McGill University, Montréal, Canada. Email: michael.rabbat@mcgill.ca.

R.D. Nowak is with the Department of Electrical and Computer Engineering, University of Wisconsin, Madison, WI, 53706. Email: nowak@engr.wisc.edu.

M.A.T. Figueiredo is with the *Instituto de Telecomunicações* and the Department of Electrical and Computer Engineering, *Instituto Superior Técnico*, Lisboa, Portugal. Email: mario.figueiredo@lx.it.pt.

linked to or from another web page, or which people were diagnosed with a common disease on the same day. Such measurements are readily available, but do not necessarily reflect the temporal or other natural order of occurrence. Researchers in this area have considered the problems of reconstructing networks from co-occurrence data and of using the inferred network to predict potential future co-occurrences [12].

Functional magnetic resonance imaging (fMRI) provides a mechanism for measuring activity in the brain with high spatial resolution. By observing which regions of the brain co-activate while a patient is performing different tasks, we can obtain multiple co-occurrence observations. Although fMRI offers high spatial resolution, its limited temporal resolution makes it impractical to obtain complete order information. Magnetoencephalography and electroencephalography measure activity in the brain with higher temporal resolution but only provide coarse spatial resolution. Consequently, these techniques do not allow a precise determination of which functional regions are active during a given task. Existing techniques for obtaining functional co-activation networks either involve brute-force measurement or use crude correlation methods (see [7] and references therein).

In this article, we focus on observations arising from transmissions in a network. Specifically, each co-occurrence observation corresponds to a path¹ through the network. We observe the vertices comprising each path but not the order in which they appear along the path. In certain applications the endpoints (source and destination) of the path may also be observed.

Our goal is to identify which pairs of vertices are directly connected via an edge, thereby learning the structure of the network. A *feasible graph* is one which agrees with the observations; *i.e.*, a graph which contains a directed path through the vertices in each co-occurrence observation. Given a collection of co-occurrence observations, a feasible graph is easily constructed by assigning an order – any order, in fact – to the vertices in each observation, and then inserting directed edges between vertices which are adjacent in the assigned order. In light of the many possible orders for each co-occurrence observation, the number of feasible topologies grows exponentially in the number and size of observations. Without additional assumptions, side information, or prior knowledge, there is no reason to prefer one feasible topology over the others.

Previous work on related problems has involved heuristics using frequencies of co-occurrence either to assign an order to each path [1] or to approximate the probability of transitioning from one vertex to another [12]. These approaches make stringent assumptions and sacrifice flexibility in order to achieve computational tractability and systematically identify a unique solution. The *frequency method* introduced in [1] is based on a model where paths from a particular source or to a particular destination form a tree. This model coincides with the shortest-path routing policy. When the network provides

multiple paths between the same pair of endpoints (*e.g.*, for load-balancing) the algorithm may fail. The *cGraph* algorithm of Kubica *et al.* [12] inserts weighted edges between every pair of vertices which co-occur in some observation. This approach produces solutions which are typically much denser than desired. Because both of these methods are based on heuristics, the results they produce are not easily interpreted. Also, these heuristics do not readily lend themselves to incorporating side information. A different approach, introduced by Justice and Hero in [13], involves averaging over an ensemble of feasible topologies sampled uniformly from the feasible set. In general there is an enormous number of feasible topologies (exponential in the problem dimensions) exhibiting a wide variety of characteristics, and it is not clear that an average of feasible topologies will be optimal in any sense. These observations have collectively motivated our development of a more general approach to network reconstruction which we simply term *network inference from co-occurrences*, or NICO for short.

Our approach is based on a generative model where paths are realizations of a random walk on the underlying graph. A co-occurrence observation is obtained by randomly shuffling each path to account for lack of observed order information. Based on this model, network inference reduces to estimating the parameters governing the random walk. Then, these parameter estimates determine the most likely order for each co-occurrence.

The following interpretation motivates our shuffled random walk model. Imagine sitting at a particular vertex in the network and observing a series of transmissions pass by. This vertex is only connected to a handful of other vertices in the network, so regardless of its final destination, a transmission arriving at this vertex must pass through one of the neighboring vertices next. By recording how many arriving transmissions are passed to each neighbor over a period of time, it is possible to calculate the empirical probability of transmission to each neighbor. Obtaining such probabilities at each vertex would provide a tremendous amount of information about the network. Unfortunately, co-occurrence observations do not directly reveal transition probabilities and we therefore face a challenging inverse problem. This paper develops a formal framework for estimating local transition probabilities from a collection of co-occurrence observations, without making any additional assumptions about routing behavior or properties of the underlying network structure. Experimental results on simulated topologies indicate that good performance is obtained for a variety of operating conditions.

A particularly novel aspect of the problem and approach introduced in this article is the counterintuitive idea of recovering temporal dynamics from non-temporal data. Models of information flow and causal signaling are quite common in problems where one is able to measure both where and when events occur. However, in the problem considered here, we have no knowledge of the temporal chain of events associated with each observation. We leverage correlation among the different activity patterns observed across the network, together with the notion that similar activity patterns are presumably caused by a common stimulus, to recover the

¹Throughout this paper a “path” refers to a sequence of vertices (x_1, x_2, \dots, x_T) such that there is an edge between each adjacent pair of vertices, x_{i-1} and x_i , and no node appears more than once in the sequence.

dynamics of information flow, a seemingly impossible task. Indeed, it is impossible to glean information about dynamics from just one co-occurrence observation, and it is only through an ensemble of patterns, which we assume are generated by the same network process, that information flow dynamics are recovered.

It is also worth mentioning that the approach discussed in this paper differs considerably from that of learning the structure of a directed graphical model or Bayesian network, a graph where nodes correspond to random variables and edges indicate conditional independence relationships [14], [15]. A typical aim of graphical modeling is to find a graph corresponding to a factorization of a high-dimensional distribution which predicts the observations well. In turn, these probabilistic models do not directly reflect physical structures, and applying such an approach in the context of this problem would ignore physical constraints inherent to the observations: that co-occurring vertices must lie along a path in the network. We note that, although the Bayesian network paradigm does not directly fit our problem setup, Teyssier and Koller [16] describe an approach to Bayesian network structure learning which is similar to the network inference algorithm presented in this paper. In [16], rather than searching over all Bayesian network structures, a search is performed over all orderings of random variables in the model. This simplifies the search procedure since it is easier to determine the mostly likely directed acyclic graph that is consistent with a fixed ordering.

The rest of the paper is organized as follows. In Section II we introduce notation and formulate the problem setup. Section III reviews the standard approach to estimating the parameters of a random walk when fully observed (ordered) samples are available and presents an EM algorithm for estimating random walk parameters from shuffled observations. A Monte Carlo variant of the EM algorithm is described in Section IV for situations where long transmission paths make the E-step computationally prohibitive. Section V analyzes convergence of the Monte Carlo EM algorithm. Simulation results are presented in Section VI and the paper is concluded in Section VII, where ongoing work is also briefly described.

II. PROBLEM FORMULATION

We model the network as a simple directed graph $G = (V, E)$, where $V = \{1, 2, \dots, |V|\}$ is the set of vertices and $E \subseteq V \times V$ is the set of edges. The number of vertices, $|V|$, is considered known, so network inference amounts to determining the adjacency structure of the graph; that is, identifying whether or not $(i, j) \in E$, for every pair of vertices $(i, j) \in V \times V$.

A co-occurrence observation, $\mathbf{x} \subset V$, is a subset of vertices in the graph which simultaneously ‘‘occur’’ when a particular stimulus is presented to the network. For example, when a transmission is made over a communication network, a subset of routers and switches carry the transmission from the source to the destination. This activated subset corresponds to a co-occurrence observation, with the stimulus being a transmission between that particular source-destination pair. By repeating this procedure N times with different stimuli

we obtain observations, $\mathbf{X} = \{\mathbf{x}^{(1)}, \mathbf{x}^{(2)}, \dots, \mathbf{x}^{(N)}\}$, where $\mathbf{x}^{(n)} = (x_1^{(n)}, x_2^{(n)}, \dots, x_{T_n}^{(n)})$ is a length- T_n co-occurrence, indexed in an arbitrary order.

A directed graph $G = (V, E)$ is said to be data-consistent with respect to observations \mathbf{X} if for each co-occurrence $\mathbf{x}^{(n)} \in \mathbf{X}$ there exists an ordered path $\mathbf{w}^{(n)} = (w_1^{(n)}, w_2^{(n)}, \dots, w_{T_n}^{(n)})$ and a permutation $\pi^{(n)} = (\pi^{(n)}(1), \dots, \pi^{(n)}(T_n))$ such that $w_t^{(n)} = x_{\pi^{(n)}(t)}^{(n)}$ for each t , and there is an edge from $w_{t-1}^{(n)}$ to $w_t^{(n)}$ in the graph for $t = 2, \dots, T_n$, that is, $(w_{t-1}^{(n)}, w_t^{(n)}) \in E$.

Notice that network inference from ordered paths is trivial. We can begin with an empty graph $G_0 = (V, E)$ with $E = \{\}$. Then, for each ordered observation $\mathbf{w}^{(n)}$ we update the set of edges via $E \leftarrow E \cup (w_{t-1}^{(n)}, w_t^{(n)})$ for $t = 2, \dots, T_n$. Even if we do not observe ordered paths, if we observe the permutation $\pi^{(n)}$ along with each co-occurrence $\mathbf{x}^{(n)}$, we can use the permutation to recover the correctly ordered observation and apply the same procedure.

In practice we do not make ordered observations and we do not have access to the correct permutations. However, we can obtain a feasible reconstruction by associating *any* permutation (of the appropriate length) with each co-occurrence, and then following the procedure described above. There are $T_n!$ ways to permute the elements of $\mathbf{x}^{(n)}$, so there may be as many as $\prod_{n=1}^N T_n!$ feasible reconstructions. Clearly, for large T_n and N this is a huge set to search over. Moreover, without making additional assumptions, or adopting some additional criteria, there is no reason to prefer one feasible reconstruction over another.

Physical principles governing the development of many natural and man-made networks suggest that not all feasible networks are equally plausible. Intuitively, if two or more vertices appear together in many co-occurrences, we expect that they are close in the underlying network topology. Likewise, we expect that most vertices will only be directly connected to a small fraction of the other vertices. Based on this intuition, we propose the following probabilistic model. First, we model the unobserved, ordered paths, $\mathbf{w}^{(n)}$, as independent samples of a first-order Markov chain. The Markov chain is parameterized by transition probabilities, $\theta_{i,j} = \mathbb{P}[w_t = j | w_{t-1} = i]$, and initial state probabilities $\theta_{0,i} = \mathbb{P}[w_1 = i]$; we denote by θ the entire collection of Markov chain parameters. Of course, these parameters must satisfy the normalization constraints,

$$\sum_{j=1}^{|V|} \theta_{i,j} = 1, \quad \text{for each } i = 0, 1, \dots, |V|. \quad (1)$$

In addition, we assume that the support of the transition matrix is determined by the adjacency structure of the underlying network; *i.e.*, $\theta_{i,j} > 0$ if and only if $(i, j) \in E$.

A co-occurrence observation, \mathbf{x} , is generated by shuffling the elements of an ordered Markov chain sample, $\mathbf{w} = (w_1, \dots, w_T)$, via a permutation π drawn uniformly from \mathbb{S}_T , the collection of all permutations of T objects. Thus, for each $t = 1, \dots, T$, $x_{\pi(t)} = w_t$. We assume the random permutation π is independent of the Markov chain sample, \mathbf{w} . Based on this model, we can write the likelihood of a co-occurrence

observation \mathbf{x} conditioned on the permutation π as

$$\mathbb{P}[\mathbf{x}|\pi, \boldsymbol{\theta}] = \theta_{0, x_{\pi(1)}} \prod_{t=2}^T \theta_{x_{\pi(t-1)}, x_{\pi(t)}}. \quad (2)$$

Since $\mathbb{P}[\pi] = 1/(T!)$, for all $\pi \in \mathbb{S}_T$, marginalization over all permutations leads to

$$\mathbb{P}[\mathbf{x}|\boldsymbol{\theta}] = \frac{1}{T!} \sum_{\pi \in \mathbb{S}_T} \mathbb{P}[\mathbf{x}|\pi, \boldsymbol{\theta}]. \quad (3)$$

Finally, assuming that co-occurrence observations are independent, and taking the logarithm, gives

$$\log \mathbb{P}[\mathbf{X}|\boldsymbol{\theta}] = \sum_{n=1}^N \left[\log \left(\sum_{\pi \in \mathbb{S}_{T_n}} \mathbb{P}[\mathbf{x}^{(n)}|\pi^{(n)}, \boldsymbol{\theta}] \right) - \log(T_n!) \right]. \quad (4)$$

Under this model, network inference consists in computing an estimate for the Markov chain parameters, $\boldsymbol{\theta}$; given a prior $\mathbb{P}[\boldsymbol{\theta}]$, a natural criterion for estimation is the maximum a posteriori criterion,

$$\hat{\boldsymbol{\theta}} = \arg \max_{\boldsymbol{\theta}} \log \mathbb{P}[\mathbf{X}|\boldsymbol{\theta}] + \log \mathbb{P}[\boldsymbol{\theta}]. \quad (5)$$

Of course, when $\mathbb{P}[\boldsymbol{\theta}]$ is a constant, independent of $\boldsymbol{\theta}$, this reduces to the maximum likelihood criterion. With the estimate $\hat{\boldsymbol{\theta}}$ in hand, we may determine the most likely permutation for each co-occurrence observation according to $\hat{\boldsymbol{\theta}}$, and obtain a feasible reconstruction using our procedure for ordered observations described above.

For non-trivial observations, $\log \mathbb{P}[\mathbf{X}|\boldsymbol{\theta}]$ is a complicated, non-concave function of $\boldsymbol{\theta}$, so solving (5) is not a simple task. In the next section, we derive a EM algorithm for finding local maxima of this optimization problem, by treating the set of permutations, $\{\pi^{(1)}, \dots, \pi^{(N)}\}$, shuffling the paths, as missing data.

III. AN EM ALGORITHM FOR ESTIMATING MARKOV CHAIN PARAMETERS FROM SHUFFLED OBSERVATIONS

A. Fully Observed Markov Chains: Notation and Estimation

Let $\mathbf{W} = \{\mathbf{w}^{(1)}, \dots, \mathbf{w}^{(T)}\}$ be a set of sample paths, $\mathbf{w}^{(n)} = (w_1^{(n)}, \dots, w_{T_n}^{(n)})$, independently generated by a Markov chain with parameters $\boldsymbol{\theta}$ (see (1)). For later use, it is convenient to introduce the equivalent binary representation $\boldsymbol{\omega}^{(n)} \in \{0, 1\}^{T_n \times |V|}$ for each sample $\mathbf{w}^{(n)}$, defined such that $\omega_{t,i}^{(n)} = \mathbb{I}_{\{w_t^{(n)}=i\}}$, where $\mathbb{I}_{\{\cdot\}}$ is the indicator function. Since $\mathbf{w}^{(n)}$ and $\boldsymbol{\omega}^{(n)}$ are equivalent representations of the same information, we will also write $\mathbf{W} \equiv \{\boldsymbol{\omega}^{(1)}, \dots, \boldsymbol{\omega}^{(N)}\}$, with a slight abuse

of notation. With this notation, we can write

$$\begin{aligned} \log \mathbb{P}[\mathbf{W}|\boldsymbol{\theta}] &= \sum_{n=1}^N \sum_{i=1}^{|V|} \omega_{1,i}^{(n)} \log \theta_{0,i} \\ &+ \sum_{n=1}^N \sum_{t=2}^{T_n} \sum_{i=1}^{|V|} \sum_{j=1}^{|V|} \omega_{t-1,i}^{(n)} \omega_{t,j}^{(n)} \log \theta_{i,j} \\ &= \sum_{i=1}^{|V|} \log \theta_{0,i} \sum_{n=1}^N \omega_{1,i}^{(n)} \\ &+ \sum_{i=1}^{|V|} \sum_{j=1}^{|V|} \log \theta_{i,j} \sum_{n=1}^N \sum_{t=2}^{T_n} \omega_{t-1,i}^{(n)} \omega_{t,j}^{(n)}. \end{aligned}$$

Maximum likelihood estimates of $\boldsymbol{\theta}$ can be obtained from \mathbf{W} by maximizing $\log \mathbb{P}[\mathbf{W}|\boldsymbol{\theta}]$ under the constraints in (1); the solution is well known,

$$\begin{aligned} \hat{\theta}_{i,j} &= \frac{\sum_{n=1}^N \sum_{t=2}^{T_n} \omega_{t-1,i}^{(n)} \omega_{t,j}^{(n)}}{|V| \sum_{n=1}^N \sum_{t=2}^{T_n} \omega_{t-1,i}^{(n)} \omega_{t,j}^{(n)}}, \quad \text{and} \\ \hat{\theta}_{0,i} &= \frac{1}{N} \sum_{n=1}^N \omega_{1,i}^{(n)}. \end{aligned} \quad (6)$$

B. Shufflings, Permutations, and the EM Algorithm

To address the case where we have a set of co-occurrences $\mathbf{X} = \{\mathbf{x}^{(1)}, \dots, \mathbf{x}^{(N)}\}$, not ordered samples, we defined the equivalent binary representation $\mathbf{X} \equiv \{\boldsymbol{\chi}^{(1)}, \dots, \boldsymbol{\chi}^{(N)}\}$ in a similar way as above: $\boldsymbol{\chi}^{(n)} \in \{0, 1\}^{T_n \times |V|}$ and $\chi_{t,i}^{(n)} = \mathbb{I}_{\{x_t^{(n)}=i\}}$.

Equivalent to using $\pi \in \mathbb{S}_T$ to denote a length- T permutation/shuffling, we introduce a more convenient (binary) representation; each shuffling is represented by a *permutation matrix*, which we also refer to as a *shuffling matrix*. Let the shuffling matrix corresponding to a permutation π be denoted as \mathbf{A}^π , where $A_{i,j}^\pi = \mathbb{I}_{\{\pi(i)=j\}}$. Thus, an ordered sequence $\boldsymbol{\omega}$, permutation π , and corresponding co-occurrence $\boldsymbol{\chi}$ are related via $\boldsymbol{\omega} = \mathbf{A}^\pi \boldsymbol{\chi}$.

Let $\Pi = \{\pi^{(1)}, \dots, \pi^{(N)}\}$ be the collection of permutations that recover the ordered paths $\mathbf{W} = \{\mathbf{w}^{(1)}, \dots, \mathbf{w}^{(T)}\}$ from the corresponding shuffled co-occurrences $\mathbf{X} = \{\mathbf{x}^{(1)}, \dots, \mathbf{x}^{(T)}\}$. Recall that the permutations, $\pi^{(m)}$, are assumed to be independent of the Markov chain parameters, $\boldsymbol{\theta}$. We can write the complete log-likelihood $\log \mathbb{P}[\mathbf{X}, \Pi|\boldsymbol{\theta}]$ as follows:

$$\begin{aligned} \log \mathbb{P}[\mathbf{X}, \Pi|\boldsymbol{\theta}] &= \log \mathbb{P}[\mathbf{X}|\Pi, \boldsymbol{\theta}] + \log \mathbb{P}[\Pi] \\ &= \sum_{n=1}^N \log \mathbb{P}[\boldsymbol{\chi}^{(n)}|\pi^{(n)}, \boldsymbol{\theta}] + \log \mathbb{P}[\Pi] \\ &= \sum_{n=1}^N \sum_{t=2}^{T_n} \sum_{t', t''=1}^{T_n} \sum_{i,j=1}^{|V|} A_{t-1,t'}^{\pi^{(n)}} A_{t,t''}^{\pi^{(n)}} \chi_{t',i}^{(n)} \chi_{t'',j}^{(n)} \log \theta_{i,j} \\ &+ \sum_{n=1}^N \sum_{t'=1}^{T_n} \sum_{i=1}^{|V|} A_{1,t'}^{\pi^{(n)}} \chi_{t',i}^{(n)} \log \theta_{0,i} + \log \mathbb{P}[\Pi], \end{aligned} \quad (8)$$

where $\mathbb{P}[\Pi]$ is the probability of the set of permutations Π , which is constant in our model since all permutations are equiprobable.

To estimate θ from \mathbf{X} , we treat Π as missing data, opening the door to the use of the EM algorithm. Notice that if we had the complete data (\mathbf{X}, Π) , we could recover \mathbf{W} via $\omega^{(n)} = \mathbf{A}^{\pi^{(n)}} \chi^{(n)}$ and obtain the closed-form estimates (6). The EM algorithm proceeds by computing the expected value of $\log \mathbb{P}[\mathbf{X}, \Pi | \theta]$ (w.r.t. Π), conditioned on the observations and on the current model estimate θ^k (the E-step),

$$Q(\theta; \theta^k) = \mathbb{E}_{\Pi} \left[\log \mathbb{P}[\mathbf{X}, \Pi | \theta] \mid \mathbf{X}, \theta^k \right], \quad (9)$$

where we write \mathbb{E}_{Π} to denote expectation with respect to the missing permutation variables, Π . The model parameter estimates are then updated as follows (the M-step):

$$\theta^{k+1} = \arg \max_{\theta} Q(\theta; \theta^k). \quad (10)$$

These two steps are repeated cyclically until a convergence criterion is met.

C. The E-step

1) *Sufficient statistics:* Rearranging (8), and dropping $\log \mathbb{P}[\Pi]$ (a constant), we can write

$$\begin{aligned} & \log \mathbb{P}[\mathbf{X}, \Pi | \theta] \\ & \propto \sum_{n=1}^N \sum_{i,j=1}^{|V|} \sum_{t',t''=1}^{T_n} \sum_{t=2}^{T_n} A_{t-1,t'}^{\pi^{(n)}} A_{t,t''}^{\pi^{(n)}} \chi_{t',i}^{(n)} \chi_{t'',j}^{(n)} \log \theta_{i,j} \\ & \quad + \sum_{n=1}^N \sum_{i=1}^{|V|} \sum_{t'=1}^{T_n} A_{1,t'}^{\pi^{(n)}} \chi_{t',i}^{(n)} \log \theta_{0,i}, \\ & = \sum_{n=1}^N \sum_{i,j=1}^{|V|} \sum_{t',t''=1}^{T_n} \alpha_{t',t''}^n \chi_{t',i}^{(n)} \chi_{t'',j}^{(n)} \log \theta_{i,j} \\ & \quad + \sum_{n=1}^N \sum_{i=1}^{|V|} \sum_{t'=1}^{T_n} \alpha_{0,t'}^n \chi_{t',i}^{(n)} \log \theta_{0,i}, \end{aligned} \quad (11)$$

revealing that $\log \mathbb{P}[\mathbf{X}, \Pi | \theta]$ is linear with respect to the following simple functions:

- the first entry of each permutation $\pi^{(n)}$: $\alpha_{0,t'}^n = A_{1,t'}^{\pi^{(n)}} = \mathbb{I}_{\{\pi^{(n)}(1)=t'\}}$, for $n = 1, \dots, N$ and $t' = 1, \dots, T_n$;
- transition indicators: $\alpha_{t',t''}^n = \sum_{t=2}^{T_n} A_{t-1,t'}^{\pi^{(n)}} A_{t,t''}^{\pi^{(n)}} = \sum_{t=2}^{T_n} \mathbb{I}_{\{\pi^{(n)}(t-1)=t'\}} \mathbb{I}_{\{\pi^{(n)}(t)=t''\}}$, for $n = 1, \dots, N$, and $t', t'' = 1, \dots, T_n$.

The E-step reduces to computing the condition expectations of $\alpha_{0,t'}^n$ and $\alpha_{t',t''}^n$ given θ^k (denoted $\bar{\alpha}_{0,t'}^{n,k}$ and $\bar{\alpha}_{t',t''}^{n,k}$), since the expectation is a linear operator and hence it commutes with linear functions. Noticing that $\alpha_{0,t'}^n$ and $\alpha_{t',t''}^n$ are binary-valued yields

$$\bar{\alpha}_{0,t'}^{n,k} = \mathbb{E} \left[\alpha_{0,t'}^n \mid \mathbf{X}, \theta^k \right] = \mathbb{P} \left[\alpha_{0,t'}^n = 1 \mid \mathbf{X}, \theta^k \right] \quad (12)$$

$$\bar{\alpha}_{t',t''}^{n,k} = \mathbb{E} \left[\alpha_{t',t''}^n \mid \mathbf{X}, \theta^k \right] = \mathbb{P} \left[\alpha_{t',t''}^n = 1 \mid \mathbf{X}, \theta^k \right] \quad (13)$$

Finally, $Q(\theta; \theta^k)$ is obtained simply by plugging $\bar{\alpha}_{0,t'}^{n,k}$ and $\bar{\alpha}_{t',t''}^{n,k}$ in the places of $\alpha_{0,t'}^n$ and $\alpha_{t',t''}^n$ in (11).

2) *Computing $\bar{\alpha}_{0,t'}^{n,k}$:* Since the permutations are (a priori) equiprobable, for $\pi \in \mathbb{S}_{T_n}$ we have $\mathbb{P}[\pi] = 1/(T_n!)$, $\mathbb{P}[\pi(1) = t'] = ((T_n - 1)!/T_n!) = 1/T_n$, and $\mathbb{P}[\pi | \pi(1) = t'] = 1/((T_n - 1)!)$. Using these facts, together with the mutual independence among the several sequences, and Bayes law, yields

$$\begin{aligned} \bar{\alpha}_{0,t'}^{n,k} &= \mathbb{P} \left[\alpha_{0,t'}^n = 1 \mid \mathbf{x}^{(n)}, \theta^k \right] \\ &= \frac{\mathbb{P}[\mathbf{x}^{(n)} | \pi^{(n)}(1) = t', \theta^k] \mathbb{P}[\pi^{(n)}(1) = t']}{\mathbb{P}[\mathbf{x}^{(n)} | \theta^k]} \\ &= \frac{\sum_{\pi \in \mathbb{S}_{T_n}: \pi(1)=t'} \mathbb{P}[\mathbf{x}^{(n)} | \pi, \theta^k]}{\sum_{\pi \in \mathbb{S}_{T_n}} \mathbb{P}[\mathbf{x}^{(n)} | \pi, \theta^k]}, \end{aligned} \quad (14)$$

where each term $\mathbb{P}[\mathbf{x}^{(n)} | \pi, \theta^k]$ is easily computed after using π to unshuffle $\mathbf{x}^{(n)}$:

$$\mathbb{P}[\mathbf{x}^{(n)} | \pi, \theta^k] = \theta_{0, x_{\pi(1)}^{(n)}}^k \prod_{t=2}^{T_n} \theta_{x_{\pi(t-1)}^{(n)}, x_{\pi(t)}^{(n)}}^k.$$

3) *Computing $\bar{\alpha}_{t',t''}^{n,k}$:* The computation of $\bar{\alpha}_{t',t''}^{n,k}$ follows a similar path as that of $\bar{\alpha}_{0,t'}^{n,k}$; since all permutations are equiprobable, for $\pi \in \mathbb{S}_{T_n}$, $\mathbb{P}[\pi(t-1) = t', \pi(t) = t''] = (T_n - 2)!/(T_n!)$ and $\mathbb{P}[\pi | \pi(t-1) = t', \pi(t) = t''] = 1/((T_n - 2)!)$, thus

$$\begin{aligned} \bar{\alpha}_{t',t''}^{n,k} &= \sum_{t=2}^{T_n} \mathbb{P}[\pi^{(n)}(t-1) = t', \pi^{(n)}(t) = t'' | \mathbf{x}^{(n)}, \theta^k] \\ &= \sum_{t=2}^{T_n} \left[\frac{\mathbb{P}[\mathbf{x}^{(n)} | \pi^{(n)}(t-1) = t', \pi^{(n)}(t) = t'', \theta^k]}{\mathbb{P}[\mathbf{x}^{(n)} | \theta^k]} \right. \\ & \quad \left. \times \mathbb{P}[\pi^{(n)}(t-1) = t', \pi^{(n)}(t) = t''] \right] \\ &= \sum_{t=2}^{T_n} \frac{\left(\frac{1}{(T_n - 2)!} \sum_{\pi \in \mathbb{S}_{T_n}: \pi(t-1)=t', \pi(t)=t''} \mathbb{P}[\mathbf{x}^{(n)} | \pi, \theta^k] \right)}{\frac{1}{T_n!} \sum_{\pi \in \mathbb{S}_{T_n}} \mathbb{P}[\mathbf{x}^{(n)} | \pi, \theta^k]} \\ & \quad \times \left(\frac{(T_n - 2)!}{T_n!} \right) \\ &= \frac{\sum_{\pi \in \mathbb{S}_{T_n}} \mathbb{P}[\mathbf{x}^{(n)} | \pi, \theta^k] \sum_{t=2}^{T_n} \mathbb{I}_{\{\pi(t-1)=t'\}} \mathbb{I}_{\{\pi(t)=t''\}}}{\sum_{\pi \in \mathbb{S}_{T_n}} \mathbb{P}[\mathbf{x}^{(n)} | \pi, \theta^k]}. \end{aligned} \quad (15)$$

Exact computation of the sufficient statistics $\{\bar{\alpha}_{0,t'}^{n,k}\}_{t'=1}^{T_n}$ and $\{\bar{\alpha}_{t',t''}^{n,k}\}_{t',t''=1}^{T_n}$ via (14) and (15) requires enumerating all permutations of $\mathbf{x}^{(n)}$. For large T_n this is a heavy load; Section IV describes a Monte Carlo sampling approach for computing approximations to $\bar{\alpha}_{0,t'}^{n,k}$ and $\bar{\alpha}_{t',t''}^{n,k}$.

D. The M-step

Recall that the function $Q(\theta; \theta^k)$ is obtained by plugging $\bar{\alpha}_{0,t'}^{n,k}$ and $\bar{\alpha}_{t',t''}^{n,k}$ in the places of $\alpha_{0,t'}^n$ and $\alpha_{t',t''}^n$, respectively,

in (11). Maximization w.r.t. θ , under the constraints in (1), leads to following simple update equations:

$$\theta_{i,j}^{k+1} = \frac{\sum_{n=1}^N \sum_{t',t''=1}^{T_n} \bar{\alpha}_{t',t''}^{n,k} \chi_{t',i}^{(n)} \chi_{t'',j}^{(n)}}{\sum_{j=1}^{|V|} \sum_{n=1}^N \sum_{t',t''=1}^{T_n} \bar{\alpha}_{t',t''}^{n,k} \chi_{t',i}^{(n)} \chi_{t'',j}^{(n)}} \quad (16)$$

and

$$\theta_{0,i}^{k+1} = \frac{\sum_{n=1}^N \sum_{t'=1}^{T_n} \bar{\alpha}_{0,t'}^{n,k} \chi_{t',i}^{(n)}}{\sum_{i=1}^{|V|} \sum_{n=1}^N \sum_{t'=1}^{T_n} \bar{\alpha}_{0,t'}^{n,k} \chi_{t',i}^{(n)}}.$$

E. Handling Known Endpoints

In some applications, (one or both of) the endpoints of each path are known and only the internal nodes are shuffled. This is the case in communication networks (*i.e.*, internally-sensed network tomography), since the sources and destinations are known, but not the connectivity within the network. In estimation of biological networks (signal transduction pathways), a physical stimulus (*e.g.*, hypotonic shock) causes a sequence of protein interactions, resulting in another observable physical response (*e.g.*, a change in cell wall structure) [3]; in this case, the stimulus and response act as fixed endpoints, our goal is to infer the order of the sequence of protein interactions.

Observe that knowledge of the endpoints of each path imposes the constraints $\pi^{(n)}(1) = 1$ and $\pi^{(n)}(T_n) = T_n$. Under the first constraint, estimates of the initial state probabilities are simply given by (for all k)

$$\theta_{0,i}^k = \frac{1}{N} \sum_{n=1}^N \chi_{1,i}^{(n)}.$$

Thus, EM only needs to be used to estimate the transition matrix entries. Let

$$\tilde{\mathbb{S}}_T = \{\pi \in \mathbb{S}_T : \pi(1) = 1, \pi(T) = T\},$$

denote the set of permutations of T elements with fixed endpoints. As in the general case, the E-step can be computed using summary statistics (for $t', t'' = 1, \dots, T_n$)

$$\tilde{\gamma}^{n,k} = \sum_{\pi \in \tilde{\mathbb{S}}_{T_n}} \mathbb{P}[\mathbf{x}^{(m)} | \pi, \theta^k]$$

$$\tilde{\gamma}_{t',t''}^{n,k} = \sum_{\pi \in \tilde{\mathbb{S}}_{T_n}} \mathbb{P}[\mathbf{x}^{(m)} | \pi, \theta^k] \sum_{t=2}^{N_m} \mathbb{I}_{\{\pi(t-1)=t'\}} \mathbb{I}_{\{\pi(t)=t''\}},$$

and setting $\bar{\alpha}_{t',t''}^{n,k} = \tilde{\gamma}_{t',t''}^{n,k} / \tilde{\gamma}$. The M-step (update for $\theta_{i,j}^{k+1}$) remains unchanged.

F. Incorporating Prior Information

The EM algorithm can be easily modified to incorporate conjugate priors; these are Dirichlet priors for each row $\theta_i =$

$(\theta_{i,1}, \dots, \theta_{i,|V|})$, $i = 0, \dots, |V|$ of θ ,

$$\mathbb{P}[\theta_i | \mathbf{u}_i] \propto \prod_{j=1}^{|V|} \theta_{i,j}^{u_{i,j}-1} \quad (17)$$

which are proper priors if and only if the parameters $u_{i,j}$ are non-negative [17]. The larger $u_{0,j}$ is relative to the other $u_{0,j'}$, $j' \neq j$, the greater our prior belief that state j is an initial state rather than the others; equivalently, the expected value of θ_0 under the Dirichlet distribution is given by $\mathbb{E}[\theta_{0,j} | \mathbf{u}_0] = u_{0,j} / \sum_{i=1}^{|V|} u_{0,i}$. Similarly, the larger $u_{i,j}$ relative to other $u_{i,j'}$ for $j' \neq j$, the more likely we expect, *a priori*, transitions from state i to state j relative to transitions from i to the other states. Consider the prior distribution on the initial state distribution; taking $u_{0,j} = c > 1$, for all j , has a *smoothing* effect, as if all of the states had some mass, regardless of the observations, in the initial state distribution.

Due to the conjugacy of the Dirichlet priors, their incorporation into the EM algorithm only results in a change to the M-step. Incorporating the prior leads to the following modified version of the function, $Q(\theta; \theta^k)$:

$$\begin{aligned} Q(\theta; \theta^k) &\propto \sum_{n=1}^N \sum_{i,j=1}^{|V|} \sum_{t',t''=1}^{T_n} \bar{\alpha}_{t',t''}^{n,k} \chi_{t',i}^{(n)} \chi_{t'',j}^{(n)} \log \theta_{i,j} \\ &+ \sum_{n=1}^N \sum_{i=1}^{|V|} \sum_{t'=1}^{T_n} \bar{\alpha}_{0,t'}^{n,k} \chi_{t',i}^{(n)} \log \theta_{0,i} \\ &+ \sum_{i,j=1}^{|V|} (u_{i,j} - 1) \log \theta_{i,j} + \sum_{i=1}^{|V|} (u_{0,i} - 1) \log \theta_{0,i}. \end{aligned} \quad (18)$$

Note that the prior does not involve the missing data (permutations) and thus does not effect the E-step calculation. The M-step updates become

$$\theta_{0,i}^{k+1} = \frac{u_{0,i} - 1 + \sum_{n=1}^N \sum_{t'=1}^{T_n} \bar{\alpha}_{0,t'}^{n,k} \chi_{t',i}^{(n)}}{\sum_{i=1}^{|V|} \left(u_{0,i} - 1 + \sum_{n=1}^N \sum_{t'=1}^{T_n} \bar{\alpha}_{0,t'}^{n,k} \chi_{t',i}^{(n)} \right)} \quad (19)$$

$$\theta_{i,j}^{k+1} = \frac{u_{i,j} - 1 + \sum_{n=1}^N \sum_{t',t''=1}^{T_n} \bar{\alpha}_{t',t''}^{n,k} \chi_{t',i}^{(n)} \chi_{t'',j}^{(n)}}{\sum_{j=1}^{|V|} \left(u_{i,j} - 1 + \sum_{n=1}^N \sum_{t',t''=1}^{T_n} \bar{\alpha}_{t',t''}^{n,k} \chi_{t',i}^{(n)} \chi_{t'',j}^{(n)} \right)} \quad (20)$$

IV. MONTE CARLO E-STEP BY IMPORTANCE SAMPLING

For long sequences, the combinatorial nature of (14) and (15) (involving sums over all permutations of each sequence) may render exact computation impractical. In this section, we consider Monte Carlo approximate versions of the E-step, which avoid the combinatorial nature of its exact version. The Monte Carlo EM (MCEM) algorithm, based on an MC version of the E-step, was originally proposed in [18], and used ever since by many authors (recent work can be found in [19]–[21] and references therein).

To lighten the notation in this section, we drop the superscript from θ^k , using simply θ as the current parameter estimates. Moreover, we focus on a particular length- T co-occurrence $\mathbf{x} = (x_1, \dots, x_T) \in V^T$ and drop the superscript (n); due to the independence of the paths, there is no loss of generality. Recall that \mathbf{x} is a (shuffled) path, and thus has no repeated elements.

The E-step (see (12) and (13)) consists of computing the conditional expectations $\bar{\alpha}_{0,t'} = \mathbb{E}[\alpha_{0,t'} | \mathbf{x}, \theta]$ and $\bar{\alpha}_{t',t''} = \mathbb{E}[\alpha_{t',t''} | \mathbf{x}, \theta]$. A naïve Monte Carlo approximation would be based on random permutations, sampled from the uniform distribution over \mathbb{S}_T . However, the reason to resort to approximation techniques in the first place is that \mathbb{S}_T is large, with only a small fraction of these random permutations having non-negligible posterior probability, $\mathbb{P}[\pi | \mathbf{x}, \theta]$; a very large number of uniform samples is thus needed to obtain a good approximation to $\bar{\alpha}_{0,t'}$ and $\bar{\alpha}_{t',t''}$.

Ideally, we would sample permutations directly from the posterior $\mathbb{P}[\pi | \mathbf{x}, \theta]$; however, this would require determining its value for all $T!$ permutations. Instead, we employ *importance sampling* (IS) (see, e.g., [22], [23], for an introduction to IS): we sample L permutations, π_1, \dots, π_L , from a distribution $\mathbb{R}[\pi | \mathbf{x}, \theta]$, from which it is easier to sample than $\mathbb{P}[\pi | \mathbf{x}, \theta]$, then apply a corrective re-weighting to obtain approximations to $\bar{\alpha}_{0,t'}$ and $\bar{\alpha}_{t',t''}$. The IS estimates are given by

$$\hat{\alpha}_{0,t'} = \frac{\sum_{i=1}^L z_i \mathbb{I}_{\{\pi_i(1)=t'\}}}{\sum_{i=1}^L z_i}, \quad (21)$$

$$\hat{\alpha}_{t',t''} = \frac{\sum_{i=1}^L z_i \sum_{t=2}^T \mathbb{I}_{\{\pi_i(t-1)=t'\}} \mathbb{I}_{\{\pi_i(t)=t''\}}}{\sum_{i=1}^L z_i}, \quad (22)$$

where z_i , the correction factor (or weight) for sample π_i , is given by

$$z_i = \frac{\mathbb{P}[\pi_i | \mathbf{x}, \theta]}{\mathbb{R}[\pi_i | \mathbf{x}, \theta]}, \quad (23)$$

the ratio between the desired distribution and the sampling distribution employed.

A relevant observation is that the target and sampling distributions only need to be known up to normalizing factors. Given $R[\pi] = Z_R \mathbb{R}[\pi | \mathbf{x}, \theta]$ and $P[\pi] = Z_P \mathbb{P}[\pi | \mathbf{x}, \theta]$, for constants Z_R and Z_P , we can use

$$z'_i = \frac{P[\pi_i]}{R[\pi_i]} = \frac{Z_P}{Z_R} z_i, \quad (24)$$

instead of z_i in (21) and (22); the approximations will remain unchanged since the factor Z_P/Z_R will appear both in the numerator and denominator of (21) and (22), thus canceling out.

The IS framework just described is general, and the performance of this approach is closely tied to the particular sampling scheme employed. In particular, the more closely the shape of the sampling distribution, \mathbb{R} , matches the shape of

the target distribution, \mathbb{P} , the better the quality of the estimate will be. Although our goal is to accurately approximate the E-step sufficient statistics, our primary motivation for using IS is to speed up calculation of the E-step. The remainder of this section describes an IS scheme which is both simple to implement (fast), and closely mimics the generative Markov model for ordered paths. Next, we describe the IS scheme, including the derivation of closed form expressions for both the sampling distribution, \mathbb{R} , and the sample weights, z_i . We conclude the section by mentioning other sampling variants.

A. Causal Sampling Scheme

Let $\mathbf{f} = \{f_1, \dots, f_{|V|}\} \in \{0, 1\}^{|V|}$ be a sequence of binary flags. Given a probability distribution $\mathbf{p} = \{p_1, p_2, \dots, p_{|V|}\}$ on the set of states, V , denote by $\mathbf{p} | \mathbf{f}$ the restriction of \mathbf{p} to those elements of V that have corresponding flag f_i set to 1, that is,

$$(\mathbf{p} | \mathbf{f})_i = \frac{p_i f_i}{\sum_{j=1}^{|V|} p_j f_j}, \quad \text{for } i = 1, 2, \dots, |V|. \quad (25)$$

The proposed sampling scheme is defined as follows:

Step 1: Let $\mathbf{f} = \{f_1, \dots, f_{|V|}\}$ be initialized according to $f_i = \mathbb{I}_{\{i \in \mathbf{x}\}}$.

Obtain one sample from V according to the distribution $\theta_0 | \mathbf{f}$. Let the obtained sample be denoted s ; of course, one and only one element of \mathbf{x} is equal to s .

Locate the position t of s in \mathbf{x} ; that is, find t such that $x_t = s$. Set $\pi(1) = t$.

Set $f_s = 0$ (preventing x_t from being sampled again).

Set $i = 2$.

Step 2: Obtain a sample s' from S , according to the distribution $\theta_s | \mathbf{f}$, where θ_s denotes the s th row of the transition matrix.

Find t such that $x_t = s'$. Set $\pi(i) = t$. Set $f_{s'} = 0$.

Step 3: If $i < N$, then set $s \leftarrow s'$, set $i \leftarrow i + 1$, go back to Step 2; otherwise, stop.

1) *Sampling Distribution*: Before deriving the form of the distribution \mathbb{R} , let us begin by writing the target distribution $\mathbb{P}[\pi | \mathbf{x}, \theta]$ explicitly. Using Bayes law,

$$\mathbb{P}[\pi | \mathbf{x}, \theta] = \frac{\mathbb{P}[\mathbf{x} | \pi, \theta] \mathbb{P}[\pi]}{\mathbb{P}[\mathbf{x} | \theta]}, \quad (26)$$

since π does not depend *a priori* on θ . Based on our assumption that all permutations are equiprobable we have $\mathbb{P}[\pi] = \mathbb{I}_{\{\pi \in \mathbb{S}_T\}}/T!$. Noticing that the denominator in (26) is just a normalizing constant independent of π , we have

$$\begin{aligned} \mathbb{P}[\pi | \mathbf{x}, \theta] &\propto \mathbb{I}_{\{\pi \in \mathbb{S}_T\}} \mathbb{P}[\mathbf{x} | \pi, \theta] \\ &= \mathbb{I}_{\{\pi \in \mathbb{S}_T\}} \left(\theta_{0, x_{\pi(1)}} \prod_{t=2}^T \theta_{x_{\pi(t-1)}, x_{\pi(t)}} \right). \end{aligned} \quad (27)$$

For the sake of notational economy, we will write simply $\mathbb{R}[\pi]$ to represent $\mathbb{R}[\pi | \mathbf{x}, \theta]$. The sequential nature of the

sampling scheme suggests a factorization of the form

$$\begin{aligned} \mathbb{R}[\pi] &= \mathbb{R}[\pi(1)] \mathbb{R}[\pi(2)|\pi(1)] \mathbb{R}[\pi(3)|\pi(2), \pi(1)] \\ &\quad \cdots \times \mathbb{R}[\pi(N)|\pi(N-1), \dots, \pi(1)]. \end{aligned} \quad (28)$$

For Step 1 of the sampling scheme, it is clear that, for $\pi(1) = 1, \dots, T$,

$$\mathbb{R}[\pi(1)] \propto \theta_{0, x_{\pi(1)}}. \quad (29)$$

For the i -th iteration, we have,

$$\begin{aligned} \mathbb{R}[\pi(i)|\pi(i-1), \dots, \pi(1)] \\ \propto \theta_{x_{\pi(i-1)}, x_{\pi(i)}} \mathbb{I}_{\{\pi(i) \notin \{\pi(i-1), \dots, \pi(1)\}\}}, \end{aligned}$$

where the indicator term simply expresses that $\pi(i)$ cannot be equal to one of the previous samples, $\pi(i-1), \dots, \pi(1)$. Observe that the normalization constant for this distribution can be expressed as

$$\sum_{j=1}^{|V|} \theta_{x_{\pi(i-1)}, j} f_j, \quad (30)$$

where $f_j = 1$ if $x_t = j$ for some $t \notin \{\pi(i-1), \dots, \pi(1)\}$. Thus, for the i -th iteration we can write

$$\begin{aligned} \mathbb{R}[\pi(i)|\pi(i-1), \dots, \pi(1)] \\ = \theta_{x_{\pi(i-1)}, x_{\pi(i)}} \phi_i(\pi(i-1), \dots, \pi(1)) \\ \times \mathbb{I}_{\{\pi(i) \notin \{\pi(i-1), \dots, \pi(1)\}\}}, \end{aligned} \quad (31)$$

with

$$\phi_i(\pi(i-1), \dots, \pi(1)) = \left(\sum_{t \notin \{\pi(i-1), \dots, \pi(1)\}} \theta_{x_{\pi(i-1)}, x_t} \right)^{-1}.$$

Inserting (29) and (31) into (28), we finally have

$$\begin{aligned} \mathbb{R}[\pi] \propto & \left[\theta_{0, x_{\pi(1)}} \prod_{t=2}^T \theta_{x_{\pi(t-1)}, x_{\pi(t)}} \right] \left[\prod_{t=2}^T \phi_t(\pi(t-1), \dots, \pi(1)) \right] \\ & \times \left[\prod_{t=2}^T \mathbb{I}_{\{\pi(t) \notin \{\pi(t-1), \dots, \pi(1)\}\}} \right]. \end{aligned} \quad (32)$$

Note that the third factor in the r.h.s. of (32) is simply the indicator that π is a permutation, *i.e.*, is equal to $\mathbb{I}_{\{\pi \in \mathcal{S}_T\}}$, for any $\pi \in \{1, \dots, T\}^T$.

Dividing (27) by (32) we obtain the correction factor z for a permutation sample π generated using this sequential scheme as

$$\begin{aligned} z &= \left(\prod_{i=2}^T \phi_i(\pi(i-1), \dots, \pi(1)) \right)^{-1} \\ &= \prod_{i=2}^T \sum_{t \notin \{\pi(i-1), \dots, \pi(1)\}} \theta_{x_{\pi(i-1)}, x_t}. \end{aligned}$$

With this quantity in hand, we have all the ingredients needed to produce IS estimates $\hat{\alpha}_{0, t'}$ and $\hat{\alpha}_{t', t''}$. Notice that computing the terms ϕ_i , and thus computing z , is easy since these factors are the normalization terms for the distributions $\theta_s | \mathbf{f}$, which are already computed while performing each iteration of Step 2. Thus, we just need to store the product of these normalizing constants to finally obtain the weight z .

2) *Known Endpoints*: In the case where the endpoints are known, we fix $\pi(1) = 1$, $\pi(T) = T$, and set $f_{x_1} = 0$ and $f_{x_T} = 0$ in Step 1; the remainder of the procedure is unchanged. Based on these constraints, the importance sampling weight takes a slightly different form:

$$z = \theta_{0, x_1} \theta_{x_{\pi(T-1)}, x_T} \prod_{i=2}^{T-1} \sum_{t \notin \{\pi(i-1), \dots, \pi(1)\}} \theta_{x_{\pi(i-1)}, x_t}. \quad (33)$$

B. Other Sampling Schemes

In addition to the causal sampling scheme that we have just described, we have also developed other sampling schemes that work in a hierarchical, rather than sequential, fashion. For the sake of space, we refrain from describing these other sampling schemes; detailed descriptions can be found in [24]. In particular, we have developed a two-stage hierarchical scheme and a fully hierarchical scheme. In the two-stage method, the first stage samples from the collection of all possible transitions occurring in a path; then the second stage samples from the distribution on all arrangements of these transitions, to form a permutation. In the fully hierarchical method, the first stage samples a suitable set of transitions, say \mathcal{G}_1 ; then, the following stage samples a suitable collection of pairs of elements of \mathcal{G}_1 , yielding a collection of quadruples, \mathcal{G}_2 , and the procedure is repeated until a permutation is obtained.

A detailed comparison of these sampling schemes with the causal sampler described above is presented in [24]. Empirically, we find that the causal sampler performs the best (lowest approximation error for a fixed number of importance samples), and so we use this sampling scheme for the remainder of the paper. Moreover, our original motivation for resorting to Monte Carlo methods was to improve the speed of computation of our algorithm. The causal sampling scheme has complexity which is linear in the length of the path to be sampled, and hence very clearly meets our needs.

V. MONOTONICITY AND CONVERGENCE

Well-known convergence results due to Wu and Boyles [25], [26] guarantee convergence of our EM algorithm when the E-step calculation is performed exactly. By choosing $\theta^{k+1} = \arg \max_{\theta} Q(\theta; \theta^k)$ in the M-step, our iterates satisfy the *monotonicity property*:

$$Q(\theta^{k+1}; \theta^k) \geq Q(\theta^k; \theta^k). \quad (34)$$

The marginal log-likelihood (4) is continuous in its parameters θ and it is bounded above. In this setting, the monotonicity property (34) guarantees that each exact EM update monotonically increases the marginal log-likelihood, so the EM iterates converge to a local maximum.

When Monte Carlo methods are used in the E-step, monotonicity is no longer guaranteed since the M-step solves $\hat{\theta}^{k+1} = \arg \max_{\theta} \hat{Q}(\theta; \theta^k)$, where \hat{Q} is defined analogously to Q but with terms $\bar{\alpha}_{t', t''}^{n, k}$ and $\bar{\alpha}_{0, t'}^{n, k}$ replaced by $\hat{\alpha}_{t', t''}^{n, k}$ and $\hat{\alpha}_{0, t'}^{n, k}$, their corresponding importance sampling approximations. Consequently, care must be taken to ensure that \hat{Q}

approximates Q well enough so that the EM algorithm is not swamped with error from the Monte Carlo estimates.

To illustrate this issue, consider the following synthetic example. We generate 40 co-occurrence observations by taking a random walk on a graph with 140 vertices. Each co-occurrence has between 4 and 8 vertices. Figure 1(a) plots $Q(\boldsymbol{\theta}^k; \boldsymbol{\theta}^{k-1})$ for the exact E-step, along with $\hat{Q}(\hat{\boldsymbol{\theta}}^{k+1}; \hat{\boldsymbol{\theta}}^k)$ and $Q(\hat{\boldsymbol{\theta}}^{k+1}; \hat{\boldsymbol{\theta}}^k)$ for the Monte Carlo EM algorithm using only 10 importance samples per co-occurrence. Although $\hat{Q}(\hat{\boldsymbol{\theta}}^{k+1}; \hat{\boldsymbol{\theta}}^k)$ increases at each iteration, $Q(\hat{\boldsymbol{\theta}}^{k+1}; \hat{\boldsymbol{\theta}}^k)$ clearly does not and the monotonicity property does not hold. This is apparent in Figure 1(b), where the dash-dot line shows the progress of the marginal log-likelihood (our optimization criterion) for the 10 sample Monte Carlo EM algorithm. When enough importance samples are used the Monte Carlo EM algorithm performs comparably to the exact EM algorithm; see the dashed line in Figure 1(b) corresponding to a Monte Carlo EM algorithm using 1000 importance samples per co-occurrence. All three instances of the EM algorithm used in this example start from the same initialization.

Recently, researchers have considered the question of how many importance samples should be used in a Monte Carlo E-step [19]–[21], [27]. The goal is to balance monotonicity and computational efficiency by using enough samples to have a good chance at monotonicity while not using excessively many samples. Booth et al. [21] argue that if the same number of importance samples is used at each EM iteration, then the algorithm will eventually be swamped by Monte Carlo error and will not converge. They also suggest requiring that a convergence criterion be satisfied on multiple successive iterations since the criterion may be met prematurely due to poor Monte Carlo approximations.

Fort and Moulines consider asymptotic convergence of Monte Carlo EM in [20]. In particular, they prove consistency of the Monte Carlo EM for curved exponential families using various forms of the ergodic theorem for Markov chains under the assumption that the number of Monte Carlo samples grows at a suitable rate with respect to the number of EM iterations.

Caffo et al. [27] propose a method for automatically adapting the number of Monte Carlo samples used at each EM iteration. Let $\Delta(\boldsymbol{\theta}^{k+1}) = Q(\boldsymbol{\theta}^{k+1}; \boldsymbol{\theta}^k) - Q(\boldsymbol{\theta}^k; \boldsymbol{\theta}^k)$ and $\hat{\Delta}(\hat{\boldsymbol{\theta}}^{k+1}) = \hat{Q}(\hat{\boldsymbol{\theta}}^{k+1}; \hat{\boldsymbol{\theta}}^k) - \hat{Q}(\hat{\boldsymbol{\theta}}^k; \hat{\boldsymbol{\theta}}^k)$. Recall that L importance samples are used to calculate the terms in \hat{Q} . The algorithm of Caffo et al. is based on a Central Limit Theorem-like approximation in which they show that $\sqrt{L}(\hat{\Delta}(\hat{\boldsymbol{\theta}}^{k+1}) - \Delta(\hat{\boldsymbol{\theta}}^{k+1}))$ converges in distribution to the standard normal. Observe that the monotonicity property (34) is equivalent to the condition $\Delta(\hat{\boldsymbol{\theta}}^{k+1}) \geq 0$. Although $\Delta(\hat{\boldsymbol{\theta}}^{k+1})$ cannot be computed without computing the exact sufficient statistics $\{\bar{\alpha}_{t', t''}^{n, k}\}$ and $\{\bar{\alpha}_{0, t'}^{n, k}\}$, we can compute $\hat{\Delta}(\hat{\boldsymbol{\theta}}^{k+1})$. Their scheme then amounts to increasing the number of Monte Carlo samples until $\hat{\Delta}(\hat{\boldsymbol{\theta}}^{k+1}) > \epsilon$ for a user-specified $\epsilon > 0$. Then, applying an asymptotic standard normal tail approximation, they obtain a statement of the form $\Pr(\hat{\Delta}(\hat{\boldsymbol{\theta}}^{k+1}) - \Delta(\hat{\boldsymbol{\theta}}^{k+1}) \geq \epsilon) \leq \delta(\epsilon)$. Based on this

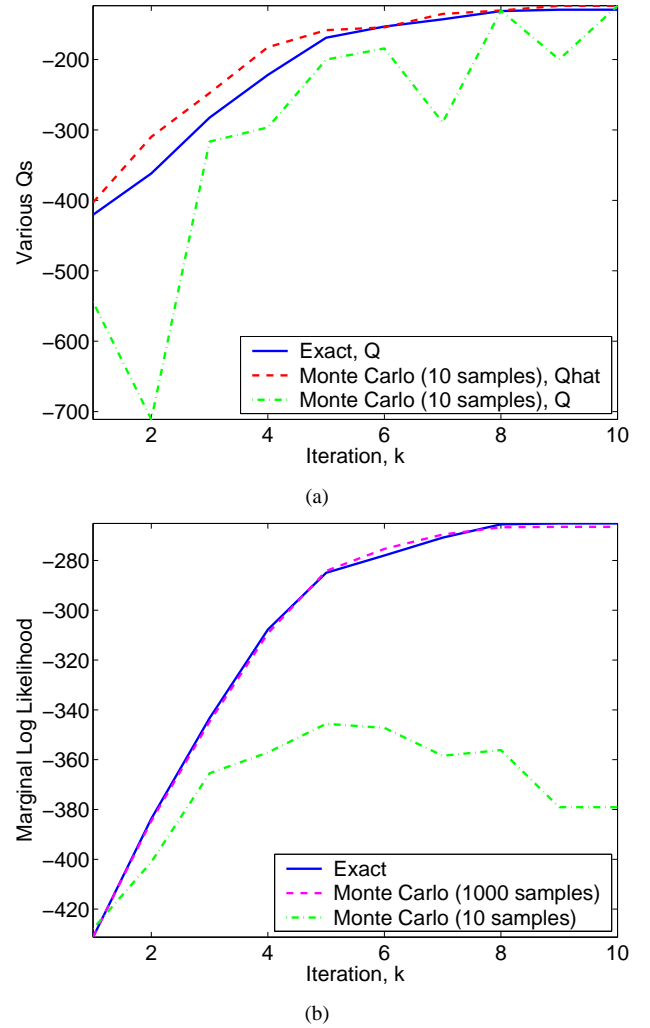


Fig. 1. An example with simulated observations illustrating that the Monte Carlo EM algorithm may not result in monotonic increase of the marginal log-likelihood if too few Monte Carlo samples are used. The solid line in (a) is $Q(\boldsymbol{\theta}^{k+1}; \boldsymbol{\theta}^k)$ for exact EM iterations, the dashed line is $\hat{Q}(\hat{\boldsymbol{\theta}}^{k+1}; \hat{\boldsymbol{\theta}}^k)$ and the dash-dot line is $Q(\hat{\boldsymbol{\theta}}^{k+1}; \hat{\boldsymbol{\theta}}^k)$ for Monte Carlo EM iterations using only 10 samples. Even though \hat{Q} increases monotonically, Q may not be monotonic for the Monte Carlo EM algorithm. Figure (b) depicts the marginal log-likelihood for exact EM iterates and for two versions of the Monte Carlo EM. Monte Carlo EM performance closely resembles that of the exact EM algorithm when sufficiently many importance samples are used.

statement they claim that monotonicity holds with probability at least $1 - \delta(\epsilon)$. They further remark that if a different ϵ_k is chosen at each iteration, so that $\sum_{k=1}^{\infty} \delta(\epsilon_k) < \infty$, then, by the Borel-Cantelli Lemma, $\Pr(\hat{\Delta}(\hat{\boldsymbol{\theta}}^k) - \Delta(\hat{\boldsymbol{\theta}}^k) \geq \epsilon_k \text{ i.o.}) = 0$, so there exists a $K > 0$ such that $\hat{\Delta}(\hat{\boldsymbol{\theta}}^k) - \Delta(\hat{\boldsymbol{\theta}}^k) < \epsilon_k$ for all $k \geq K$ with probability 1; *i.e.*, eventually every EM update is monotonic. Of course, in practice, the algorithm is terminated after a finite number of iterations, so we may never reach the stage where all iterates are monotonic.

Notice that for the monotonicity condition $\Delta(\hat{\boldsymbol{\theta}}^{k+1}) \geq 0$ to truly hold in the above framework, the events

$$\left\{ \hat{\Delta}(\hat{\boldsymbol{\theta}}^{k+1}) - \Delta(\hat{\boldsymbol{\theta}}^{k+1}) \leq \epsilon \right\} \quad \text{and} \quad \left\{ \hat{\Delta}(\hat{\boldsymbol{\theta}}^{k+1}) \geq \epsilon \right\}$$

must occur simultaneously. Because the probabilistic bound

above only addresses one of these events we refer to this type of result as guaranteeing an (ϵ, δ) -*probably approximately monotonic* update, or PAM for short. More generally, an (ϵ, δ) -PAM result states that with probability at least $1 - \delta$, the update will be ϵ -approximately monotonic; i.e., $\widehat{\Delta}(\widehat{\boldsymbol{\theta}}^{k+1}) - \Delta(\widehat{\boldsymbol{\theta}}^{k+1}) \leq \epsilon$ implies $\Delta(\widehat{\boldsymbol{\theta}}^{k+1}) \geq -\epsilon$, because, by definition, $\widehat{\Delta}(\widehat{\boldsymbol{\theta}}^{k+1}) \geq 0$.

Rather than resorting to asymptotic approximations to obtain such a result, we can take advantage of the specific form of Q in our problem to obtain the finite-sample PAM result presented next. Recall that independent importance samples are drawn for each co-occurrence observation in the Monte Carlo E-step. Denote by L_n the number of importance samples used to compute sufficient statistics for observation $\mathbf{x}^{(n)}$. The computational complexity of the exact E-step computation for this observation requires $T_n!$ operations (enumerating all permutations of $\mathbf{x}^{(n)}$), and thus increases with the size of the co-occurrence. Similarly, we should expect that larger observations will require more importance samples for two reasons: 1) there are more sufficient statistics associated with this observation (T_n^2 in total), and 2) there are more ways to shuffle these observations.

In the previous section we derived closed form expressions for the importance sample weights, $z_i = \mathbb{P}[\pi_i | \mathbf{x}, \boldsymbol{\theta}] / \mathbb{R}[\pi_i | \mathbf{x}, \boldsymbol{\theta}]$, where \mathbb{P} is the target distribution and \mathbb{R} is the importance sampling distribution. A key assumption was made that \mathbb{P} is absolutely continuous with respect to \mathbb{R} ; that is, $\mathbb{P}[\pi | \mathbf{x}, \boldsymbol{\theta}] = 0$ for every permutation π with $\mathbb{R}[\pi | \mathbf{x}, \boldsymbol{\theta}] = 0$. We adopt the convention $0/0 = 0$ so that $z_i = 0$ for such samples. This guarantees that $z_i < \infty$. The bounds below depend on the quality of our importance sample estimators as gauged by

$$b_n = \max_{\pi \in \mathbb{S}_{T_n}} \frac{\mathbb{P}[\pi | \mathbf{x}^{(n)}, \boldsymbol{\theta}]}{\mathbb{R}[\pi | \mathbf{x}^{(n)}, \boldsymbol{\theta}]} \quad (35)$$

Because the set \mathbb{S}_{T_n} is finite, $\mathbb{P}[\pi | \mathbf{x}^{(n)}, \boldsymbol{\theta}]$ and $\mathbb{R}[\pi | \mathbf{x}^{(n)}, \boldsymbol{\theta}]$ have finite support, and the maximum is well-defined (finite). If \mathbb{R} matches the target distribution \mathbb{P} well then b_n should not be very large.

There is one other subtlety that we must introduce for our bounds. Because the terms of $\widehat{Q}(\boldsymbol{\theta}; \boldsymbol{\theta}^k)$ have factors $\log \theta_{i,j}$ and $\log \theta_{0,i}$, in practice we typically bound $\theta_{i,j}$ and $\theta_{0,i}$ away from zero to ensure that \widehat{Q} does not go to $-\infty$. This is easily accomplished with a Dirichlet prior, as discussed after the theorem below. Thus, for the theorem we will assume that $\theta_{i,j}^k \geq \theta_{\min}$ and $\theta_{0,i}^k \geq \theta_{\min}$ for some $0 < \theta_{\min} < |V|^{-1}$. The upper bound on θ_{\min} ensures it is still possible to satisfy the constraints (1).

We have the following finite-sample PAM result for our Monte Carlo EM algorithm.

Theorem 1: Let $\epsilon > 0$ and $\delta > 0$ be given and assume there exists $\theta_{\min} \in (0, |V|^{-1})$ such that $\theta_{i,j}^k \geq \theta_{\min}$ and $\theta_{0,i}^k \geq \theta_{\min}$ for all i and j . If

$$L_n = \frac{2N^2 T_n^4 b_n^2 |\log \theta_{\min}|^2}{\epsilon^2} \log \left(\frac{2T_n^2}{1 - (1 - \delta)^{1/T}} \right) \quad (36)$$

importance samples are used for the m th observation then $\widehat{\Delta}(\widehat{\boldsymbol{\theta}}^{k+1}) - \Delta(\widehat{\boldsymbol{\theta}}^{k+1}) < \epsilon$ with probability greater than $1 - \delta$.

The proof of Theorem 1 appears in Appendix . Because $\widehat{\Delta}(\widehat{\boldsymbol{\theta}}^{k+1}) \geq 0$ by definition, the theorem guarantees that $\Delta(\widehat{\boldsymbol{\theta}}^{k+1}) > -\epsilon$ with probability greater than $1 - \delta$.

Remark 1: If the EM algorithm is initialized with $\theta_{i,j}^0 > 0$ (i.e., all entries initialized with positive values), then all finite iterates will also be bounded away from zero. However, the iterates may tend arbitrarily close to zero, violating the assumption of the theorem. This problem can be resolved by using a Dirichlet prior with $u_{i,j} = c > 1$, for all i, j , effectively adding a bit of mass to all possible transitions (see Section III-F for discussion of priors). For example, taking $c = 2$ has the effect of assuming one observation of each and every transition. The prior places a small amount of mass on every transition, and results in EM iterates that satisfy the lower bound $\theta_{\min} := \frac{1}{|V|(1+N)}$. Recalling the M-step formula using the Dirichlet prior (19) and taking $u_{0,i} = 2$ for all i produces

$$\theta_{0,i}^{k+1} = \frac{1 + \sum_{n=1}^N \sum_{t'=1}^{T_n} \bar{\alpha}_{0,t'}^{n,k} \chi_{t',i}^{(n)}}{\sum_{i=1}^{|V|} \left(1 + \sum_{n=1}^N \sum_{t'=1}^{T_n} \bar{\alpha}_{0,t'}^{n,k} \chi_{t',i}^{(n)} \right)} \geq \frac{1}{|V|(1+N)}$$

where the inequality follows by noting that the minimum of the numerator is 1 and the denominator is bounded above by $|V|(1+N)$ since all the summands of $\sum_{n=1}^N \sum_{t'=1}^{T_n} \bar{\alpha}_{0,t'}^{n,k} \chi_{t',i}^{(n)}$ lie in the set $[0, 1]$, and for each n at most one $\chi_{t',i}^{(n)}$, $t' = 1, \dots, T_n$ is non-zero. A similar bounding argument shows that $\theta_{i,j}^{k+1} \geq \frac{1}{|V|(1+N)}$ when $u_{i,j} = 2$ for all i, j . Observe that the incorporation of the prior does not alter the proof of Theorem 1 since the prior terms (i.e., log of the Dirichlet prior) in $\widehat{\Delta}(\widehat{\boldsymbol{\theta}}^{k+1})$ and $\Delta(\widehat{\boldsymbol{\theta}}^{k+1})$ are independent of the sufficient statistics and thus cancel each other. Note that this choice of prior results in the following requirement on the number of importance samples

$$L_n \geq \frac{2N^2 T_n^4 b_n^2 [\log(|V|(1+N))]^2}{\epsilon^2} \log \left(\frac{2T_n^2}{1 - (1 - \delta)^{1/N}} \right). \quad (37)$$

Finally, we also point out that if two vertices i and j do not co-occur in any of the observations, then one can set $\theta_{i,j}^0 = 0$, effectively eliminating it from further consideration. This will not affect the EM algorithm or the bounds above. However, if one suspects that the observations do not necessarily reflect all possible paths, then it may be sensible to use the Dirichlet prior in such situations.

Recall that exact E-step computation requires $T_n!$ operations for the n th observation. The bound above stipulates that the number of importance samples required is proportional to $T_n^4 \log T_n^2$. Generating one importance sample using the causal sampling scheme requires T_n operations, and thus, the computational complexity of a PAM Monte Carlo update only depends on $T_n^5 \log T_n^2$, which clearly demonstrates that the computational complexity of the Monte Carlo E-step depends polynomially on T_n in comparison to exponential dependence for the exact E-step.

To put this result in perspective, observe that the value of L_n given by (36) is roughly a factor of N away from the value we would expect based on an asymptotic variance calculation. Ignoring constants and log terms, for fixed θ we have

$$\begin{aligned} \text{Var}(\widehat{\Delta}(\theta)) &\approx \text{Var}\left(\sum_{n=1}^N \sum_{t',t''=1}^{T_n} \widehat{\alpha}_{t',t''}^{n,k} + \sum_{n=1}^N \sum_{t'=1}^{T_n} \widehat{\alpha}_{0,t'}^{n,k}\right) \\ &= \sum_{n=1}^N \text{Var}\left(\sum_{t',t''=1}^{T_n} \widehat{\alpha}_{t',t''}^{n,k} + \sum_{t'=1}^{T_n} \widehat{\alpha}_{0,t'}^{n,k}\right), \end{aligned}$$

since independent sets of importance samples are used to calculate sufficient statistics for different observations. It is easily shown that the variance of an individual approximate statistic $\widehat{\alpha}_{t',t''}^{n,k}$ or $\widehat{\alpha}_{0,t'}^{n,k}$ decays according to the parametric rate; *i.e.*, $\text{Var}(\widehat{\alpha}_{t',t''}^{n,k}) = O(1/L_n)$. In total, there are T_n^2 sufficient statistics for the n th observation, and they are all potentially correlated since they are functions of the same set of importance samples. Then we have

$$\text{Var}(\widehat{\Delta}(\theta)) = O\left(\sum_{n=1}^N \frac{(T_n^2)}{L_n}\right).$$

To drive $\text{Var}(\widehat{\Delta}(\theta))$ down to a constant level, independent of N and T_n , we need $L_n \propto NT_n^4$. The additional factor of N in our bound is essentially an artifact from the union bound.

Note that if we use different δ_k at each EM iteration, chosen such that $\sum_{k=1}^{\infty} \delta_k < \infty$, then by the Borel-Cantelli Lemma one can argue that $\Pr(\Delta(\widehat{\theta}^k) < 0 \text{ i.o.}) = 0$. In other words, eventually all EM iterates result in a monotonic increase of the marginal log-likelihood.

In addition to demonstrating that the Monte Carlo EM algorithm has polynomial computational complexity, this bound gives a useful guideline for determining how many importance samples should be used. However, because they involve worst-case analysis, the number of samples dictated by this bound tends to be on the conservative side. For example, in the Internet experiments described in Section VI, $N = 249$ and the average path length is 17 hops. Theorem 1 suggests that roughly 10 billion importance samples should be used per observation. However, in our experiments we find that the algorithm exhibits reasonable performance on this data set using as few as 2,000 samples per observation. Of course, in practice, the only way to know the value of b_n is to enumerate all permutations, so this bound cannot be used as an explicit guideline.

VI. EXPERIMENTAL RESULTS

In this section, we evaluate the performance of our *network inference from co-occurrences* (NICO) algorithm on simulated data and on data gathered from the public Internet. In the results reported below, network reconstructions are obtained by first estimating an initial state distribution and probability transition matrix via the EM algorithm. Then, we compute the most likely order of each observation according to the inferred model and use this ordering to reconstruct a feasible network. The EM algorithm cannot be guaranteed to converge to a

global maximum (the marginal log-likelihood is not concave) and there may even be multiple global maxima. To address this issue, we rerun the EM algorithm from multiple random initializations and report the collective results.

We compare the performance of our algorithm with that of the *frequency method* (FM), defined in [1] and mentioned in Section I. The FM also reconstructs a network topology by estimating an order of the vertices in each observation. This method individually determines each path ordering independently by sorting the elements in the path according to how correlated each vertex is with the endpoints of the path. It is possible that multiple vertices may receive identical FM scores, in which case their sorting would be arbitrary (one could exchange elements with identical scores without violating the FM criteria). In fact, we observe this phenomenon in many of our experiments. Ties are resolved by choosing a random order for elements with identical scores. Multiple restarts are also performed using the FM, yielding a collection of feasible solutions.

The quality of a network reconstruction is determined by a quantity we term the *edge symmetric difference* error. Because the nodes in the network have unique labels, the goal of any reconstruction scheme is to determine which vertices are connected by an edge. The edge symmetric difference error is defined as the sum of the number of false positives (edges appearing in the reconstructed network which do not exist in the true network) and the number of false negatives (edges in the true network not appearing in the reconstructed network).

A. Simulated Networks

Our synthetic data is obtained as described next. A network is generated according to a random geometric graph model: 50 vertices are thrown at random in the unit square, and two vertices are connected with an edge if the Euclidean distance between them is less than or equal to $\sqrt{\log(50)}/50$. This threshold guarantees that the graph is connected with high probability [28]. Groups of nodes are randomly chosen as sources and destinations, transmission paths are generated between each source-destination pair according to either a shortest path or random routing model, and then co-occurrence observations are formed from each path. We keep the number of sources fixed at 5 and vary the number of destinations between 5 and 40, to see how the number of observations effects performance. Each experiment is repeated on 100 different topologies, using 10 restarts of both NICO and the FM per configuration. Exact E-step calculation is used for observations with $T_n \leq 12$, and causal importance sampling (2000 samples) is used for longer paths. The longest observation in our data was obtained by random routing and has $T_n = 19$ (notice that $19! \approx 10^{17}$). No prior is used in any of the results reported here. In our experience, we found little practical difference between the MLE and the MAP estimate based on a Dirichlet prior with $u_{i,j} = 2$, as discussed in Remark 1.

Figure 2 plots edge symmetric difference performance for synthetic data generated using (a) shortest path routing and (b) random routing. The edge symmetric difference error is computed between the inferred network and the graph obtained

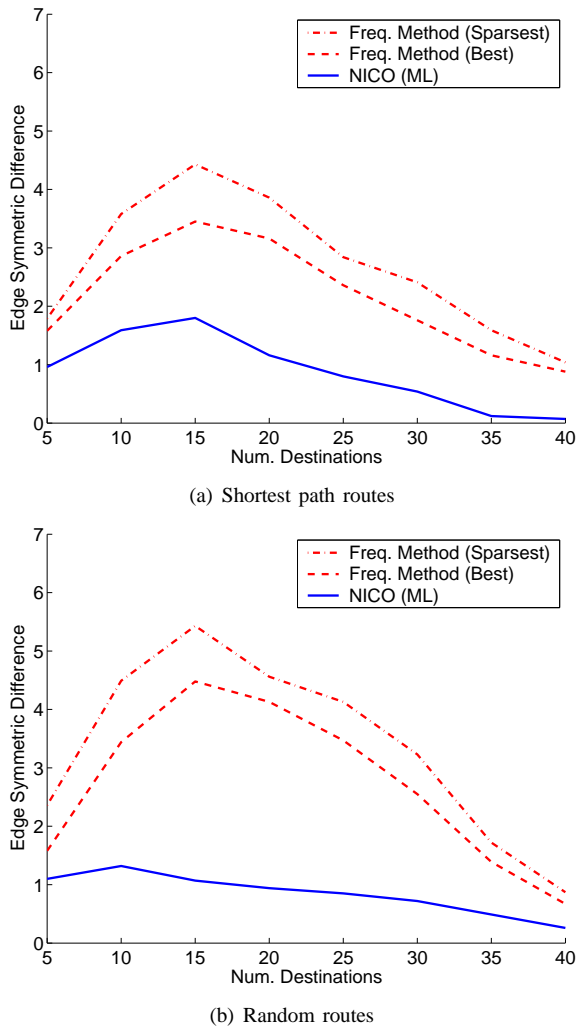


Fig. 2. Edge symmetric differences between inferred networks and the network one would obtain using co-occurrence measurements arranged in the correct order. Performance is averaged over 100 different network configurations. For each configuration 10 NICO and FM solutions are obtained via different initializations. We then choose the NICO solution yielding the largest likelihood, and compare with both the sparsest and clairvoyant best FM solution.

from correctly ordered observations. Of the 10 solutions corresponding to different NICO initializations, we use the one based on parameter estimates yielding the highest likelihood score. For this simulation, the most likely NICO solution also always resulted in the best edge symmetric difference error.

The FM does not provide a similar mechanism for ranking different solutions. A possible heuristic would be to choose the sparsest solution (with fewest edges). The figures show performance for both this heuristic, and clairvoyantly choosing the best (lowest error) solution of the 10. In fact, using the sparsest solution does better than just choosing a FM solution at random but not as well as using the clairvoyant best. In these simulations, NICO consistently outperform the FM.

Notice that both algorithms exhibit their worst performance at an intermediate number of destinations. When very few destinations are used the measured topology closely resembles a tree, regardless of the underlying routing mechanism. Relative frequencies of co-occurrence accurately reflect the network

distance of each internal vertex from the path endpoints. At the other extreme, when many destinations are used, there is significant overlap among the co-occurrence observations which aids in localizing vertices. In general, the FM seems to be much more sensitive to the amount of data available.

As expected, the FM generally performs better on shortest path data than it does on random routes. When routes are generated randomly the corresponding topology is less tree-like and pair-wise co-occurrence frequencies do not reflect network distances. Because NICO is not based on a particular routing paradigm it performs similarly in both scenarios, possibly even a little better when routing is random.

B. Internet Data

We have also studied the performance of our algorithm on co-occurrence observations gathered from the Internet. Using `traceroute` we have collected data describing roughly 250 router-level paths from sources at the University of Wisconsin-Madison, the *Instituto Superior Técnico* in Lisbon, and Rice University to 83 servers affiliated with corporations, universities, and governments around the world. Our motivation for using this type of data is two-fold. First, `traceroute` allows us to measure the true order of elements in each path so that we have a ground truth to validate our results against. Second, and more importantly, the data comes from a real network where, presumably, paths are not generated according to a first-order Markov model. This allows us to gauge the robustness of the proposed model and to evaluate how well it generalizes to realistic scenarios. The ground truth network contains a total of 1105 nodes and 1317 edges, and the longest observed path has length 27.

For this data set we rerun FM and NICO each from 50 random initializations and look at performance across all solutions rather than focusing on the maximum likelihood or clairvoyant best. The exact E-step is used to compute sufficient statistics for paths of up to 9 hops. For paths longer than 9 hops, we use the causal importance sampling described in Section IV-A, with 2000 samples per observation.

Minimum, median, and maximum edge symmetric difference errors are shown in Figure 3. Both algorithms have seemingly high error rates, as there are roughly 1300 links in the true network. However keep in mind that both algorithms are attempting to fill in the entries of a roughly 1100×1100 matrix. For 50 networks constructed by choosing a random order for the elements of each observation the average edge symmetric difference error was 4300, so both algorithms are indeed doing considerably better than random guessing. NICO performance is again noticeably better than that of the FM; the NICO average error is better than that of the best FM reconstruction, and the worst case NICO reconstruction is on par with the average FM performance. We also note that the number of false positives and false negatives in a reconstruction using either scheme tend to be roughly equal (each constituting half of the edge symmetric difference error).

Figure 4 shows statistics for the number of edges in the reconstructed networks. There is an interesting correlation between the number of edges and reconstruction accuracy in

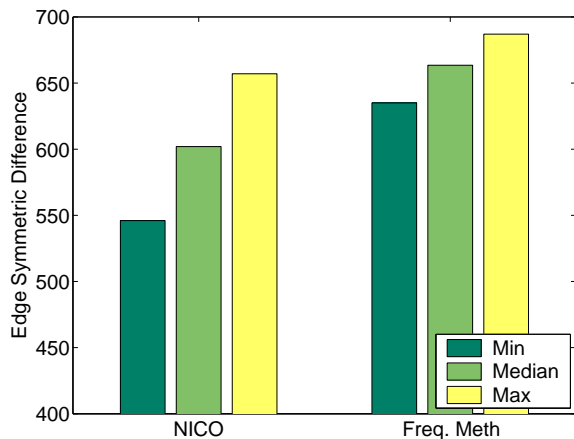


Fig. 3. Edge symmetric difference error comparison of NICO and FM on Internet data. The reported values come from 50 random initializations of each algorithm.

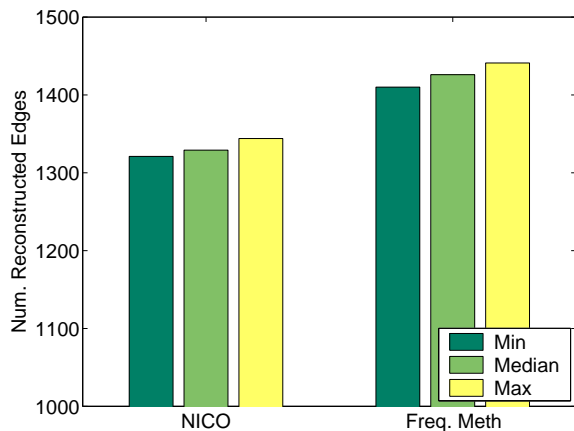


Fig. 4. Number of edges in networks reconstructed using each method. The median number of edges per reconstruction is 1329 for NICO and 1426 for FM. The true network has 1317 edges, and so it appears that NICO does a better job of capturing the complexity of the true network.

this example. As seen above, the typical NICO reconstruction is more accurate, in terms of edge errors, than a FM reconstruction. NICO also consistently returns a sparser estimate. The median number of links in a NICO reconstruction is 1329, whereas the median number of links in a FM reconstruction is 1426. There are 1317 edges in the true network, so in this sense the NICO reconstructions more accurately reflect the inherent level of complexity in the true network.

Marginal log-likelihood values for each of the 50 NICO estimates are depicted in Figure 5. The marginal log-likelihood, given by (4), is the cost function being optimized by the EM algorithm. In contrast to the experiments with simulated data reported above, there is no exact correlation between higher marginal likelihood values and lower edge symmetric difference error for this example. The topology with the highest likelihood value results in an edge symmetric difference error of 627. This is better than the clairvoyant best FM error, but only average for NICO. The three repetitions which returned a topology with the lowest symmetric difference error had the next highest likelihood value, as indicated by the three hollow

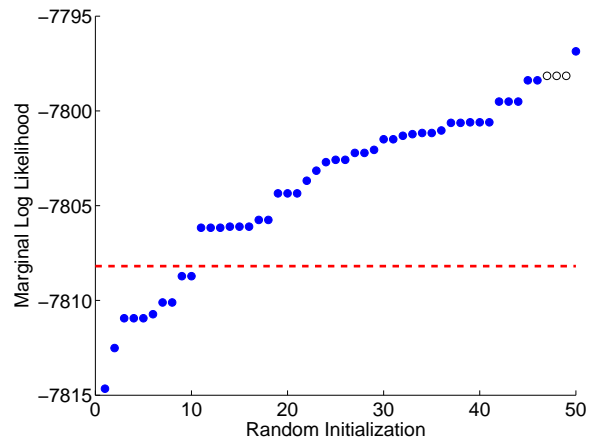


Fig. 5. Marginal log likelihood values for different random initializations of NICO, sorted in ascending order. The three hollow circles correspond to the solutions which achieve the lowest edge symmetric difference error of all NICO trials. The dashed line shows the marginal log likelihood value computed using the true path orders to estimate a Markov transition matrix. Most NICO solutions have higher marginal log-likelihood than the true topology, suggesting that our generative model does not accurately describe Internet topology data.

circles in the figure. The dashed line shows the likelihood value based on a transition matrix estimated using the true path orders as measured by `traceroute`. Notice that the majority of the NICO solutions have a higher marginal likelihood than the true topology. This suggests that our generative model may not be the best match for Internet topology data. Still the overall performance of our algorithm is encouraging.

VII. DISCUSSION AND ONGOING RESEARCH

This paper presents a novel approach to network inference from co-occurrence observations. A co-occurrence observation reflects which vertices are activated by a particular transmission through the network, but not the order in which they are activated. We model transmission paths as random walks on the underlying graph structure. Co-occurrence observations are modeled as i.i.d. samples of the random walk subjected to a random permutation which accounts for the lack of observed path order. Treating the random permutations as latent variables we derive an *expectation-maximization* (EM) algorithm for efficiently computing maximum likelihood or maximum *a posteriori* estimates of the random walk parameters (initial state distribution and transition matrix).

The complexity of the EM algorithm is dominated by the E-step calculation which is exponential in the length of the longest transmission path. In order to handle large networks, we describe fast approximation methods based on importance sampling and Monte Carlo techniques. We derive concentration-style bounds on the accuracy of the Monte Carlo approximation. These bounds prescribe how many importance samples must be used to ensure a monotonic increase in the log-likelihood, thereby guaranteeing convergence of the algorithm with high probability. The resulting Monte Carlo EM computational complexity only depends polynomially on the length of the longest path.

To obtain a network reconstruction, we determine the most likely order for each co-occurrence observation according to the Markov chain parameter estimates, and then insert edges in the graph based on these ordered transmission paths. This procedure always produces a feasible reconstruction. The parameter estimates produced by the EM algorithm may be useful for other tasks such as guiding an expert to alternative reconstructions by assigning likelihoods to different permutations, or predicting unobserved paths through the network as in [13]. One could also analyze properties of an ensemble of solutions obtained by running the EM algorithm from different initializations, and then posit a new set of experiments to be conducted based on this analysis.

The transition matrix parameter $\theta_{i,j}$ can be interpreted as estimates of the probability that a transmission will be passed from vertex i to j , conditioned on the path reaching i ; that is, $\theta_{i,j} = \mathbb{P}[w_{k+1} = j | w_k = i]$. In particular, they are *not* estimates of the probability of a link existing from i to j . Since θ is a stochastic matrix, each row must sum to 1, and so if vertex i is connected to many other nodes then the unit mass is being spread over more entries. We can obtain joint probabilities, $\mathbb{P}[w_k = i, w_{k+1} = j]$, via Bayes theorem,

$$\mathbb{P}[w_{k+1} = j | w_k = i] = \frac{\mathbb{P}[w_k = i, w_{k+1} = j]}{\mathbb{P}[w_k = i]},$$

where $\mathbb{P}[w_k = i]$ is the stationary distribution of the chain (not necessarily equal to the initial state distribution). These joint probabilities (appropriately scaled versions of the transition matrix entries) more accurately reflect the likelihood of there being an edge from i to j , based on our estimates.

Our future work involves extending and generalizing both algorithmic and theoretical aspects of this work. In our experiments we found that our current model leads to reasonable Internet reconstructions, but we feel there is room for improvement. For example, the structure of Internet paths may depend strongly on the destination of the traffic. In fact, one could partition the co-occurrence data into source-dependent (or destination-dependent) subsets and learn different Markov models for each subset (see, e.g., [29]). However, if two or more sources (respectively, destinations) have similar routes, then one could potentially obtain a better overall estimate by pooling observations from the sources. We are currently investigating models based on “mixtures of random walks” to account for this added level of dependency. Nevertheless, although the source-dependent model more accurately reflects how routing is performed in actual communication systems, there are scenarios where a single transition matrix estimate is preferable. For example, a more holistic characterization of network routing is valuable if one is interested in predicting the route between a source and destination that was not previously observed, or if one is interested in predicting the endpoints of a route given only the activated internal routers [13].

Co-occurrence observations naturally arise from transmission *paths* in communication network applications and, to a degree, in biological, social, and brain networks as well. However the physical mechanisms driving interactions in the latter three applications may also correspond to more general connected subgraph structures such as trees or directed acyclic

graphs. Extending our methods in this fashion is easily accomplished in theory, however the computational complexity may be significantly increased when more general structures are considered.

In this paper we have also restricted our attention to noise-free observations. We are also interested in extending our algorithm to handle the case where observations reflect a soft probability that a given vertex occurred in the path rather than hard, “active” or “not active”, binary observations. This extension is relevant in many applications including the inference of signal transduction networks (in systems biology) where co-occurrence observations are themselves the result of inference procedures run on experimental data.

APPENDIX

There are two main steps in the proof of Theorem 1. First, we derive a concentration inequality for the importance sample approximations, $\hat{\alpha}_{i',i''}^{n,k}$ and $\hat{\alpha}_{0,i'}^{n,k}$. Then we use the inequality to construct a bound for $\hat{\Delta}(\hat{\theta}^{k+1}) - \Delta(\theta^{k+1})$.

Recall the expressions (21) and (22) for importance sample approximations calculated in the Monte Carlo E-step. Both are of the general form $\hat{\mu}_L = \frac{\sum_{i=1}^L Z(\pi_i)X(\pi_i)}{\sum_{i=1}^L Z(\pi_i)}$, where $Z : \mathbb{S}_T \rightarrow [0, b]$ and $X : \mathbb{S}_T \rightarrow \{0, 1\}$, and they are approximating $\mu = \sum_{\pi \in \mathbb{S}_T} X(\pi) \mathbb{P}[\pi | \mathbf{x}, \theta]$. The permutations π_1, \dots, π_L are i.i.d. samples from the distribution $\mathbb{R}[\pi | \mathbf{x}, \theta]$. Note that $\mathbb{E}[\hat{\mu}_L] \neq \mu$, so standard concentration results such as Hoeffding’s inequality or McDiarmid’s bounded-differences inequality do not directly apply; e.g., consider the case $L = 1$:

$$\mathbb{E} \left[\frac{Z(\pi_1)X(\pi_1)}{Z(\pi_1)} \right] = \sum_{\pi \in \mathbb{S}_T} X(\pi) \mathbb{R}[\pi | \mathbf{x}, \theta] \quad (38)$$

$$\neq \sum_{\pi \in \mathbb{S}_T} X(\pi) \mathbb{P}[\pi | \mathbf{x}, \theta]. \quad (39)$$

We can, however, show that $\hat{\mu}_L$ yields an asymptotically consistent estimate of μ . Observe that

$$\mathbb{E}[Z(\pi_i)] = \sum_{\pi \in \mathbb{S}_T} \frac{\mathbb{P}[\pi | \mathbf{x}, \theta]}{\mathbb{R}[\pi | \mathbf{x}, \theta]} \mathbb{R}[\pi | \mathbf{x}, \theta] \quad (40)$$

$$= 1, \quad (41)$$

since \mathbb{P} is a probability distribution on \mathbb{S}_T , and

$$\mathbb{E}[Z(\pi_i)X(\pi_i)] = \sum_{\pi \in \mathbb{S}_T} \frac{\mathbb{P}[\pi | \mathbf{x}, \theta]}{\mathbb{R}[\pi | \mathbf{x}, \theta]} X(\pi) \mathbb{R}[\pi | \mathbf{x}, \theta] \quad (42)$$

$$= \sum_{\pi \in \mathbb{S}_T} X(\pi) \mathbb{P}[\pi | \mathbf{x}, \theta] \quad (43)$$

$$= \mu. \quad (44)$$

It follows from the strong law of large numbers that $\hat{\mu}_L \rightarrow \mu$ as $L \rightarrow \infty$.

The following finite-sample concentration inequality demonstrates that the approximation error, $\hat{\mu}_L - \mu$, decays exponentially in the number of importance samples, L .

Proposition 1: Let $\{(X_i, Z_i)\}$ be a sequence of independent and identically distributed random variables with $X_i \in \{0, 1\}$ and $Z_i \in [0, b]$. Assume that $\mathbb{E}[Z_i] = 1$ and $\mathbb{E}[Z_i X_i] =$

μ , and set $\hat{\mu}_L = \frac{\sum_{i=1}^L Z_i X_i}{\sum_{i=1}^L Z_i}$. Then with probability greater than $1 - \delta$,

$$\hat{\mu}_L - \mu < \sqrt{\frac{2b^2 \log \frac{2}{\delta}}{L}}. \quad (45)$$

Proof: From the definitions of Z_i and X_i , $Z_i X_i \in [0, b]$. Applying Hoeffding's inequality [30] yields that for any $t > 0$,

$$\Pr\left(\sum_{i=1}^L Z_i X_i - L\mu \geq Lt\right) \leq e^{-2Lt^2/b^2}, \quad (46)$$

and for any $t > 0$,

$$\Pr\left(\sum_{i=1}^L Z_i - L \leq -Lt\right) \leq e^{-2Lt^2/b^2}. \quad (47)$$

Define the event, $E_t = \left\{\sum_{i=1}^L Z_i X_i - L\mu \geq Lt\right\} \cup \left\{\sum_{i=1}^L Z_i - L \leq -Lt\right\}$.

By the union bound, $\Pr(E_t) \leq 2e^{-2Lt^2/b^2}$ for any $t > 0$. The complement of E_t implies that for $t \in (0, 1)$,

$$\hat{\mu}_L - \mu = \frac{\sum_{i=1}^L Z_i X_i - L\mu}{\sum_{i=1}^L Z_i} + \frac{L\mu}{\sum_{i=1}^L Z_i} - \mu \quad (48)$$

$$< \frac{Lt}{L(1-t)} + \frac{L\mu}{L(1-t)} - \mu \quad (49)$$

$$= \frac{t(1+\mu)}{1-t}. \quad (50)$$

It follows that $\left\{\hat{\mu}_L - \mu \geq \frac{t(1+\mu)}{1-t}\right\} \subseteq E_t$, and so $\Pr\left(\hat{\mu}_L - \mu \geq \frac{t(1+\mu)}{1-t}\right) \leq \Pr(E_t) \leq 2e^{-2Lt^2/b^2}$. Since $\hat{\mu}_L \leq 1$, if $\frac{t(1+\mu)}{1-t} + \mu > 1$ then $\Pr\left(\hat{\mu}_L - \mu \geq \frac{t(1+\mu)}{1-t}\right) = 0$, and the proposition holds trivially. Thus, without loss of generality we consider the case $\frac{t(1+\mu)}{1-t} + \mu \leq 1$, or equivalently, $t \leq (1-\mu)/2$. This restriction on t implies $\frac{t(1+\mu)}{1-t} \leq 2t$, and so we have $\Pr(\hat{\mu}_L - \mu < 2t) > 1 - 2e^{-2Lt^2/b^2}$. Set $\delta = 2e^{-2Lt^2/b^2}$ to obtain the desired result. \blacksquare

We apply Proposition 1 to the Monte Carlo approximations $\{\hat{\alpha}_{t',t''}^{n,k}\}$ and $\{\hat{\alpha}_{0,t'}^{n,k}\}$ as follows. Recall that the Monte Carlo weights are bounded according to $z_i \in [0, b_n]$, with b_n as defined in (35). Define the event

$$B_{\delta',L_n}^n = \left(\bigcup_{\substack{t',t''=1 \\ t' \neq t''}}^{T_n} \left\{ \hat{\alpha}_{t',t''}^{n,k} - \bar{\alpha}_{t',t''}^{n,k} \geq \sqrt{\frac{2b_n^2 \log \frac{2}{\delta'}}{L_n}} \right\} \right) \cup \left(\bigcup_{t'=1}^{T_n} \left\{ \hat{\alpha}_{0,t'}^{n,k} - \bar{\alpha}_{0,t'}^{n,k} \geq \sqrt{\frac{2b_n^2 \log \frac{2}{\delta'}}{L_n}} \right\} \right).$$

This is a union over $2\binom{T_n}{2} + T_n = T_n^2$ events, each of which holds with probability at most δ' according to Proposition 1. By the union bound it follows that $\Pr(B_{\delta',L_n}^n) \leq T_n^2 \delta'$. Next, let C_{δ',L_n}^n denote the event that

$$\sum_{t',t''=1}^{T_n} \left(\hat{\alpha}_{t',t''}^{n,k} - \bar{\alpha}_{t',t''}^{n,k} \right) + \sum_{t'=1}^{T_n} \left(\hat{\alpha}_{0,t'}^{n,k} - \bar{\alpha}_{0,t'}^{n,k} \right) \geq T_n^2 \sqrt{\frac{2b_n^2 \log \frac{2}{\delta'}}{L_n}},$$

and observe that $C_{\delta',L_n}^n \subseteq B_{\delta',L_n}^n$, therefore $\Pr(C_{\delta',L_n}^n) \leq \Pr(B_{\delta',L_n}^n) \leq T_n^2 \delta'$. Let $\delta'' = T_n^2 \delta'$ and let $L > 0$ be a value to be determined later. For each $n = 1, \dots, N$, set

$$L_n = \frac{2LT_n^4 b_n^2 \log \frac{2T_n^2}{\delta''}}{\log \frac{1}{\delta''}}, \quad (51)$$

so that

$$T_n^2 \sqrt{\frac{2b_n^2 \log \frac{2}{\delta'}}{L_n}} = T_n^2 \sqrt{\frac{2b_n^2 \log \frac{2T_n^2}{\delta''}}{L_n}} = \sqrt{\frac{\log \frac{1}{\delta''}}{L}}. \quad (52)$$

Then with probability greater than $1 - \delta''$,

$$\sum_{t',t''=1}^{T_n} \left(\hat{\alpha}_{t',t''}^{n,k} - \bar{\alpha}_{t',t''}^{n,k} \right) + \sum_{t'=1}^{T_n} \left(\hat{\alpha}_{0,t'}^{n,k} - \bar{\alpha}_{0,t'}^{n,k} \right) < \sqrt{\frac{\log \frac{1}{\delta''}}{L}}. \quad (53)$$

Recall that $\chi_{t',i}^{(n)}$ are indicator variables satisfying $\sum_{i,j=1}^{|V|} \chi_{t',i}^{(n)} \chi_{t',j}^{(n)} = 1$ and $\sum_{i=1}^{|V|} \chi_{t',i}^{(n)} = 1$. Multiplying each term in (53) by the appropriate sum of indicators, rearranging terms, and recalling that importance sample estimates for different observations are statistically independent, we have that with probability greater than $(1 - \delta'')^T$,

$$\bigcap_{n=1}^N \left\{ \sum_{t',t''=1}^{T_n} \sum_{i,j=1}^{|V|} \left(\hat{\alpha}_{t',t''}^{n,k} - \bar{\alpha}_{t',t''}^{n,k} \right) \chi_{t',i}^{(n)} \chi_{t',j}^{(n)} + \sum_{t'=1}^{T_n} \sum_{i=1}^{|V|} \left(\hat{\alpha}_{0,t'}^{(n)} - \bar{\alpha}_{0,t'}^{(n)} \right) \chi_{t',i}^{(n)} < \sqrt{\frac{\log \frac{1}{\delta''}}{L}} \right\},$$

which implies that with probability greater than $(1 - \delta'')^N$,

$$\sum_{n=1}^N \sum_{t',t''=1}^{T_n} \sum_{i,j=1}^{|V|} \left(\hat{\alpha}_{t',t''}^{n,k} - \bar{\alpha}_{t',t''}^{n,k} \right) \chi_{t',i}^{(n)} \chi_{t',j}^{(n)} + \sum_{n=1}^N \sum_{t'=1}^{T_n} \sum_{i=1}^{|V|} \left(\hat{\alpha}_{0,t'}^{n,k} - \bar{\alpha}_{0,t'}^{n,k} \right) \chi_{t',i}^{(n)} < N \sqrt{\frac{\log \frac{1}{\delta''}}{L}}.$$

Finally, set $1 - \delta = (1 - \delta'')^T$ and multiply through by $|\log \theta_{\min}| > 0$. Then with probability greater than $1 - \delta$,

$$\sum_{n=1}^N \sum_{t',t''=1}^{T_n} \sum_{i,j=1}^{|V|} \left(\hat{\alpha}_{t',t''}^{n,k} - \bar{\alpha}_{t',t''}^{n,k} \right) \chi_{t',i}^{(n)} \chi_{t',j}^{(n)} |\log \theta_{\min}| + \sum_{n=1}^N \sum_{t'=1}^{T_n} \sum_{i=1}^{|V|} \left(\hat{\alpha}_{0,t'}^{n,k} - \bar{\alpha}_{0,t'}^{n,k} \right) \chi_{t',i}^{(n)} |\log \theta_{\min}| < N |\log \theta_{\min}| \sqrt{\frac{-\log(1 - (1 - \delta)^{1/N})}{L}}. \quad (54)$$

To complete the proof, observe that

$$\begin{aligned} & \widehat{\Delta}(\widehat{\theta}^{k+1}) - \Delta(\widehat{\theta}^{k+1}) \\ &= \sum_{n=1}^N \sum_{i,j=1}^{|V|} \sum_{t',t''}^{T_n} \left(\widehat{\alpha}_{t',t''}^{n,k} - \bar{\alpha}_{t',t''}^{n,k} \right) \chi_{t',i}^{(n)} \chi_{t'',j}^{(n)} \left(\log \widehat{\theta}_{i,j}^{k+1} - \log \theta_{i,j}^k \right) \\ & \quad + \sum_{n=1}^N \sum_{i=1}^{|V|} \sum_{t'=1}^{T_n} \left(\widehat{\alpha}_{0,t'}^{n,k} - \bar{\alpha}_{0,t'}^{n,k} \right) \chi_{t',i}^{(n)} \left(\log \widehat{\theta}_{0,i}^{k+1} - \log \theta_{0,i}^k \right). \end{aligned} \quad (55)$$

By assumption, $\theta_{\min} \leq \theta_{i,j}^k \leq 1$ for each $(i,j) \in V^2$. It follows that

$$\log \widehat{\theta}_{i,j}^{k+1} - \log \theta_{i,j}^k \leq -\log \theta_{\min} = |\log \theta_{\min}|. \quad (56)$$

Similarly, $\log \widehat{\theta}_{0,i}^{k+1} - \log \theta_{0,i}^k \leq |\log \theta_{\min}|$ for each $i \in V$. Apply these bounds in (55) to find that the right hand side of (55) is no greater than the left hand side of (54). Set

$$\epsilon = N |\log \theta_{\min}| \sqrt{\frac{\log \frac{1}{1-(1-\delta)^{1/N}}}{L}}. \quad (57)$$

Then $\widehat{\Delta}(\widehat{\theta}^{k+1}) - \Delta(\widehat{\theta}^{k+1}) < \epsilon$ with probability greater than $1 - \delta$. Solve for L in (57) and plug the resulting value back into (51) with $\delta'' = 1 - (1 - \delta)^{1/N}$ to obtain the desired result.

REFERENCES

- [1] M. G. Rabbat, J. R. Treichler, S. L. Wood, and M. G. Larimore, "Understanding the topology of a telephone network via internally-sensed network tomography," in *Proc. IEEE International Conference on Acoustics, Speech, and Signal Processing*, vol. 3, Philadelphia, PA, March 2005, pp. 977–980.
- [2] M. Coates, A. O. Hero, R. Nowak, and B. Yu, "Internet tomography," *IEEE Signal Processing Magazine*, vol. 19, no. 3, pp. 47–65, 2002.
- [3] E. Klipp, R. Herwig, A. Kowald, C. Wierling, and H. Lehrach, *Systems Biology in Practice: Concepts, Implementation and Application*. John Wiley and Sons, 2005.
- [4] B. O. Palsson, *Systems Biology: Properties of Reconstructed Networks*. Cambridge University Press, 2006.
- [5] S. Wasserman, K. Faust, D. Iacobucci, and M. Granovetter, *Social Network Analysis: Methods and Applications*. Cambridge University Press, 1994.
- [6] M. Newman, A. L. Barabasi, and D. J. Watts, *The Structure and Dynamics of Networks*. Princeton University Press, 2006.
- [7] O. Sporns and G. Tononi, "Classes of network connectivity and dynamics," *Complexity*, vol. 7, no. 1, pp. 28–38, 2002.
- [8] O. Sporns, D. R. Chialvo, M. Kaiser, and C. C. Hilgetag, "Organization, development and function of complex brain networks," *Trends in Cognitive Science*, vol. 8, no. 9, 2004.
- [9] *International Workshop on Brain Connectivity*, 2005, <http://www.ccs.fau.edu/~bc2005/welcome.html>.
- [10] D. Zhu, A. O. Hero, H. Cheng, R. Khanna, and A. Swaroop, "Network constrained clustering for gene microarray data," *Bioinformatics*, vol. 21, no. 21, pp. 4014–4020, 2005.
- [11] Y. Liu and H. Zhao, "A computational approach for ordering signal transduction pathway components from genomics and proteomics data," *BMC Bioinformatics*, vol. 5, no. 158, October 2004.
- [12] J. Kubica, A. Moore, D. Cohn, and J. Schneider, "cGraph: A fast graph-based method for link analysis and queries," in *Proc. IJCAI Text-Mining and Link-Analysis Workshop*, Acapulco, Mexico, August 2003.
- [13] D. Justice and A. O. Hero, "Estimation of message source and destination from link intercepts," *IEEE Trans. on Information Forensics and Security*, vol. 1, no. 3, pp. 374–385, September 2006.
- [14] D. Heckerman, D. Geiger, and D. Chickering, "Learning Bayesian networks: The combination of knowledge and statistical data," *Machine Learning*, vol. 20, pp. 197–243, 1995.
- [15] N. Friedman and D. Koller, "Being Bayesian about Bayesian network structure: A Bayesian approach to structure discovery in Bayesian networks," *Machine Learning*, vol. 50, no. 1–2, pp. 95–125, 2003.
- [16] M. Teyssier and D. Koller, "Ordering-based search: A simple and effective algorithm for learning Bayesian networks," in *Proc. Conference on Uncertainty in AI*, Edinburgh, Scotland, July 2005.
- [17] J. Bernardo and A. Smith, *Bayesian Theory*. John Wiley & Sons, 1994.
- [18] G. C. G. Wei and M. A. Tanner, "A Monte Carlo implementation of the EM algorithm and the poor mans data augmentation algorithms," *Journal of the American Statistical Association*, vol. 85, pp. 699–704, 1990.
- [19] W. Jank, "Stochastic variants of the EM algorithm: Monte Carlo, quasi-Monte Carlo and more," in *Proc. of the American Statistical Association*, Minneapolis, Minnesota, August 2005.
- [20] G. Fort and E. Moulines, "Convergence of the Monte Carlo expectation maximization for curved exponential families," *Annals of Statistics*, vol. 31, no. 4, pp. 1220–1259, 2003.
- [21] J. G. Booth, J. P. Hobert, and W. S. Jank, "A survey of Monte Carlo algorithms for maximizing the likelihood of a two-stage hierarchical model," *Statistical Modelling*, vol. 1, pp. 333–349, 2001.
- [22] C. Robert and G. Casella, *Monte Carlo Statistical Methods*. New York: Springer Verlag, 1999.
- [23] J. S. Liu, *Monte Carlo Strategies in Scientific Computing*. Springer, 2001.
- [24] M. G. Rabbat, M. A. T. Figueiredo, and R. D. Nowak, "Network inference from co-occurrences," April 2006, technical report ECE-06-02, Department of Electrical and Computer Engineering, University of Wisconsin-Madison.
- [25] C. F. J. Wu, "On the convergence properties of the EM algorithm," *Annals of Statistics*, vol. 11, no. 1, pp. 95–103, 1983.
- [26] R. A. Boyles, "On the convergence of the EM algorithm," *Journal of the Royal Statistical Society B*, vol. 45, no. 1, pp. 47–50, 1983.
- [27] B. S. Caffo, W. Jank, and G. L. Jones, "Ascent-based Monte Carlo EM," *Journal of the Royal Statistical Society B*, vol. 67, no. 2, pp. 235–252, 2005.
- [28] P. Gupta and P. Kumar, "The capacity of wireless networks," *IEEE Transactions on Information Theory*, vol. 46, no. 2, pp. 388–404, March 2000.
- [29] D. Justice and A. Hero, "Online methods for network endpoint localization," April 2007, submitted to *IEEE Transactions on Information Theory*.
- [30] W. J. Hoeffding, "Probability inequalities for sums of bounded random variables," *Journal of the American Statistical Association*, vol. 58, pp. 713–721, 1963.